Journal of Medicinal Chemistry

Article

pubs.acs.org/jmc

Creation of Customized Bioactivity within a 14-Membered Macrolide Scaffold: Design, Synthesis, and Biological Evaluation Using a Family-18 Chitinase

Akihiro Sugawara,[†,⊥] Nobuo Maita,[‡,⊥,#] Hiroaki Gouda,[§,⊥] Tsuyoshi Yamamoto,[†] Tomoyasu Hirose,[†] Saori Kimura,[†] Yoshifumi Saito,[†] Hayato Nakano,[†] Takako Kasai,[†] Hirofumi Nakano,[†] Kazuro Shiomi,[†] Shuichi Hirono,[§] Takeshi Watanabe,[∥] Hisaaki Taniguchi,[‡] Satoshi Ōmura,*[,†] and Toshiaki Sunazuka*[,†]

[†]The Kitasato Institute, Kitasato Institute for Life Sciences and Graduate School of Infection Control Sciences, Kitasato University, 5-9-1, Shirokane, Minato-ku, Tokyo 108-8641, Japan

[‡]Institute for Enzyme Research, University of Tokushima, 3-18-15 Kuramotocho, Tokushima City, Tokushima, 770-8503, Japan

[§]School of Pharmacy, Kitasato University, 5-9-1, Shirokane, Minato-ku, Tokyo 108-8641, Japan

[∥]Department of Applied Biological Chemistry, Faculty of Agriculture, Niigata University, 8050 Ikarashi-2, Niigata 950-2181, Japan

Supporting Information

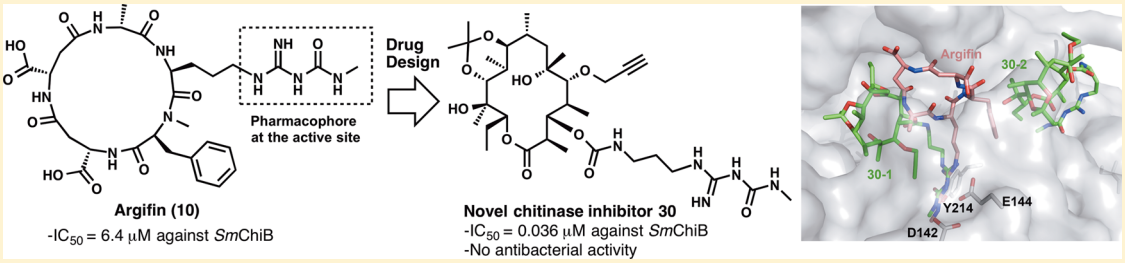

ABSTRACT: Argifin, a 17-membered pentapeptide, inhibits chitinase. As argifin has properties that render it unsuitable as a drug development candidate, we devised a mechanism to create the structural component of argifin that bestows the chitinase inhibition and introduce it into a 14-membered macrolide scaffold. Here we describe (1) the designed macrolide, which exhibits ~200-fold more potent chitinase inhibition than argifin, (2) the binding modes of the macrolide with *Serratia marcescens* chitinase B, and (3) the computed analysis explaining the reason for derivatives displaying increased inhibition compared to argifin, the macrolide aglycone displaying inhibition in a nanomolar range. This promises a class of chitinase inhibitors with novel skeletons, providing innovative insight for drug design and the use of macrolides as adaptable, flexible templates for use in drug discovery research and development.

INTRODUCTION

Although 14-membered macrolides, such as erythromycin A (**1**, Figure 1),[1] are widely recognized as antibacterial agents,[2] they also display gastrointestinal motor-stimulating (GMS) activity[3] and anti-inflammatory and/or immunomodulatory activity.[4] Currently, 14-membered macrolides are used for the treatment of diffuse panbronchiolitis as anti-inflammatory and/or immunomodulatory agents.[5] Several research groups have been investigating the development of nonantibiotic macrolides derived from **1**[6,7] to help prevent development of antibiotic resistance. Our research group has already developed nonantibiotic macrolides derived from **1**, both EM574 (**2**),[8−11] as a motilin agonist, and EM900 (**3**)[12] with anti-inflammatory and/or immunomodulatory effects (Figure 1), and we believe that 14-membered macrolides could be useful templates for drug discovery.[13]

Chitinase hydrolyzes chitin, a homopolymer of *N*-acetylglucosamine (GlcNAc), a key structure of fungal cell walls, cuticles of insects, and microfilarial sheaths in parasitic nematodes but absent from all mammalian cells.[14−16] Although chitinases are classified as family-18 and family-19 based on amino acid similarity,[17,18] family-18 chitinases are connected with inflammatory and infectious diseases and have been utilized as molecular targets.[19] Interestingly, two types of family-18 chitinases, namely, acidic mammalian chitinase (AMCase), expressed in human epithelial cells of lower airways, and human chitotriosidase (HCHT), expressed in phagocytes, have been identified in mammalian cells[20] despite the fact that humans do not metabolize chitin. More importantly, in 2004, inhibitors of AMCase reduced infiltrate of eosinophilic lung disease in T-cell mediated inflammation.[21] Consequently, chitinase inhibitors are expected to be potential drugs for the treatment of asthma. Moreover, other chitinase-like proteins, known as chi-lectins, have been implicated in Th2-driven pathology.[22] Other diseases, such as atherosclerosis, juvenile idiopathic arthritis,

Received: January 30, 2015

DOI: 10.1021/acs.jmedchem.5b00175
J. Med. Chem. XXXX, XXX, XXX−XXX

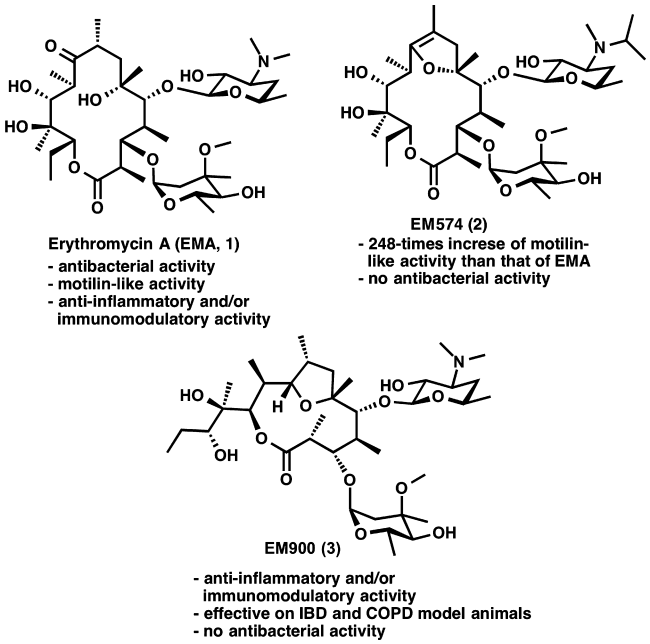

Figure 1. Structures of erythromycin A (EMA) (**1**), EM574 (**2**), and EM900 (**3**).

and Alzhheimer's disease, have been linked with chitinases. Recently, Janda and co-workers reported that inhibition of a family-18 chitinase from *Onchocerca volvulus* may provide a new therapy against onchocerciasis (river blindness).[23,24] However, the role of chitinase in mammalian cells is not fully understood. As such, revealing the true role of chitinases in humans may provide significant health benefits.

Given the attractive potential of chitinases, several natural-product inhibitors have been reported, such as allosamidin (**4**),[25,26] styloguanidine (**5**),[27] 3-bromostyloguanidine (**6**), 2,3-dibromostyloguanidine (**7**), Cl-4 (**8**),[28−30] and psammaplin (**9**)[31,32] (Figure 2).[19] Our research group has also reported two naturally occurring chitinase inhibitors, argifin (**10**)[33−35] and argadin (**11**)[36] (Figure 2). The two potent cyclic pentapeptide chitinase inhibitors, **10** and **11**, were isolated from the culture broth of *Gliocladium sp.* FTD-0668 and *Clonostachys* sp. FO-7314, respectively, and found to be potent inhibitors of *Serratia marcescens* chitinases (*Sm*ChiB; IC_{50} = 6.4 μM and 0.033 μM, respectively).[37] To date, the only natural product chitinase inhibitor possessing the *N*-methylcarbamoylguanidinyl group is **10**. Therefore, its mode of action is of considerable interest. X-ray crystallographic analysis[38,39] revealed that the *N*-methylcarbamoylguanidinyl group is located in the tunnel-like active site pocket through a hydrogen bonding network between the family-18 chitinase, *Sm*ChiB (Asp142, Glu144, and Tyr214), and the argifin ligand (see Figure 5B). This finding indicates that the *N*-methylcarbamoylguanidinyl group functions as the "pharmacophore" as an anchor motif in family-18 chitinases. Inspired by this observation, van Aalten, Eggleston, and co-workers[40−42] reported the total synthesis, analog synthesis, and dissection analogs of argifin. Independently, our group[43−49] also reported the total synthesis of argifin-based analogs through computer-aided molecular design and in situ click chemistry applications.[37,50,51]

Although several natural or synthetic chitinase inhibitors having different skeletons have been reported, none of the known inhibitors have been clinically utilized because of several factors, such as synthetic inaccessibility, cost performance, and unsuitable properties. These limitations indicate that a novel chitinase inhibitor with a new skeleton would be extremely useful. Some of the unfavorable drug properties of **10** were a

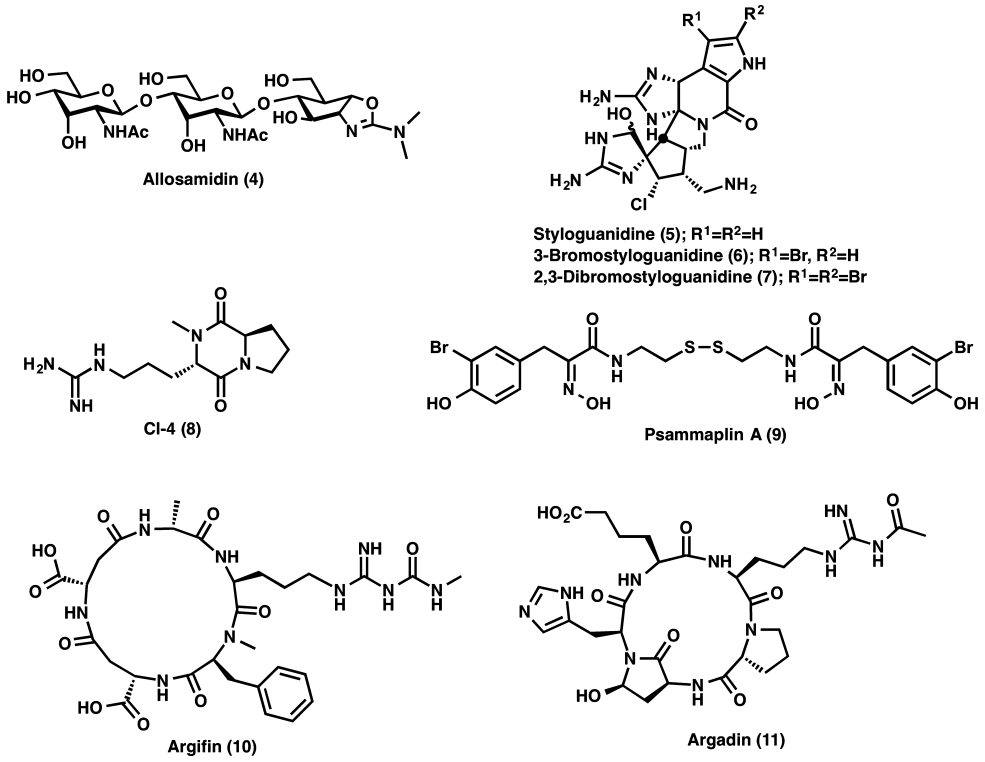

Figure 2. Natural-product chitinase inhibitors.

DOI: 10.1021/acs.jmedchem.5b00175
J. Med. Chem. XXXX, XXX, XXX−XXX

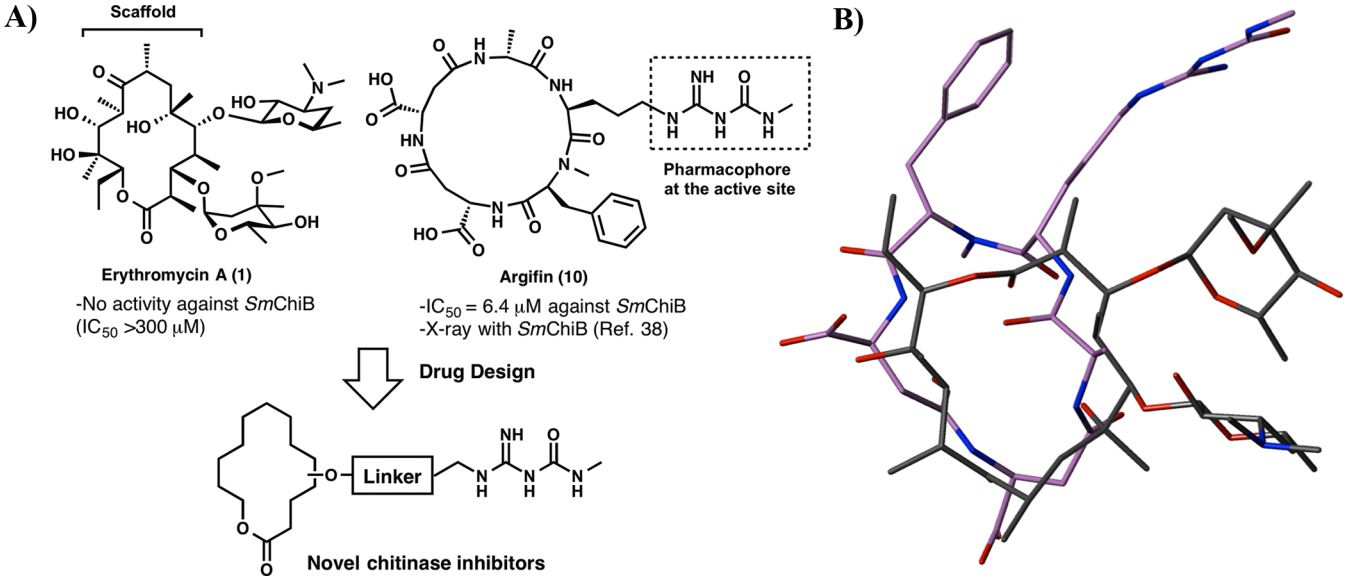

Figure 3. Drug design inspired by structures of erythromycin A (**1**) and argifin (**10**): (A) strategy for creating novel chitinase inhibitors; (B) aligned three-dimensional structures of **1** (gray) and **10** (purple).

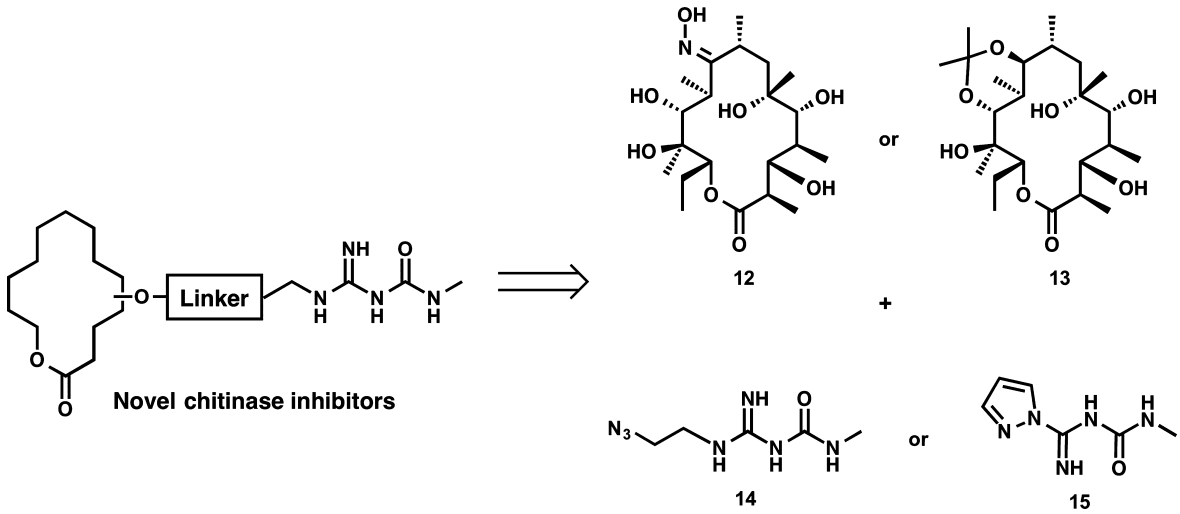

Figure 4. Strategy for synthesizing novel chitinase inhibitors.

low value of clogP (−2.24), which might affect bioavailability, synthetic inaccessibility, and limited scope for modifying the peptide side chain. To address these issues, our strategy was to assemble the key structural features responsible for chitinase inhibition into a macrolide scaffold devoid of inherent bioactivity, especially antibacterial activity. In other words, we wanted to replace the cyclic peptide backbone skeleton of **10** with that of the aglycone found in **1** (Figure 3A), as we speculated that the three-dimensional (3D) structure of **1** might resemble **10** in NMR spectroscopy and X-ray crystallography, as seen in our previous studies (Figure 3B).[38,52,53]

In early peptidomimetic studies, Hirschmann[54,55] reported that a sugar backbone can mimic *β*-turn analogs of cyclic peptides. More recently, Randolph and Oyelere independently reported that 14- and 15-membered macrolides can be replaced with cyclic peptides while maintaining biological activity.[56−58] However, to the best of our knowledge, no literature has been published on the chitinase inhibitor argifin. The advantages of our strategy are the variation of the physicochemical properties of **10**, development of a process to manipulate chemical structures to induce desired bioactive properties, and full use of the potential and pharmacological advantages offered by the distinctive properties of **1**. In this study, we used *Sm*ChiB as a model enzyme for family-18 chitinases. Herein, we report the design, synthesis, and in vitro biological evaluation of customized 14-membered macrolides with acquired chitinase inhibitory activity. In addition, we reveal their binding mechanisms by determination of the series of crystal structures of *Sm*ChiB complexed with 14-membered macrolides with 2.0−2.6 Å resolution, allowing creation of a logical chitinase inhibitor design.

■ RESULTS AND DISCUSSION

Synthesis and Biological Activity of Chitinase Inhibitors with 14-Membered Macrolides. On the basis of our strategy, we anticipated that suitable starting materials would be erythronolide A oxime (**12**) and (9*S*)-9-dihydro-9,11-*O*-isopropylideneerythronolide A (**13**), which were prepared from **1** in two-[59] and eight-step processes, respectively (Figure

DOI: 10.1021/acs.jmedchem.5b00175
J. Med. Chem. XXXX, XXX, XXX−XXX

Scheme 1. Synthesis of Azide 14 and Pyrazole Carboxamidine 15 Possessing *N*-Methylcarbamoylguanidino Moiety[a]

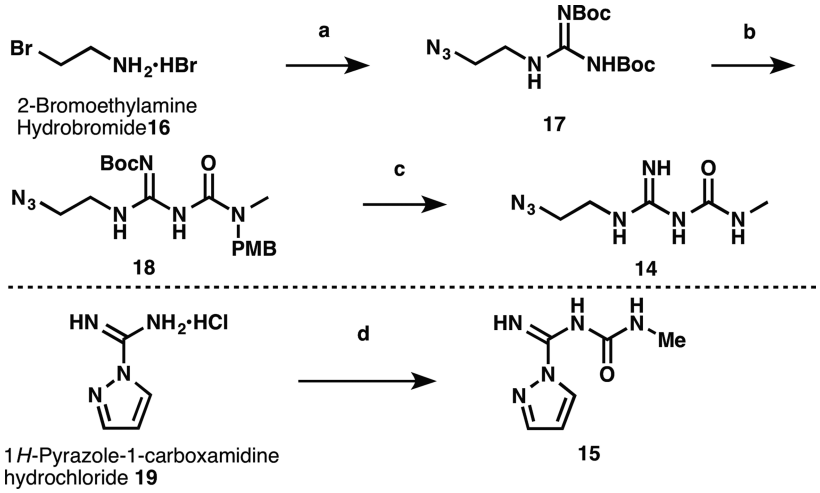

[a]Reagents and conditions: (a) NaN_3, H_2O, then *N*,*N*′-di-Boc-1*H*-pyrazole-1-carboxamidine, DIPEA, MeCN, rt, 15 h, 94% (2 steps); (b) *N*-methyl-*p*-methoxybenzylamine, THF, reflux, 16 h, 91%; (c) 90% TFA in DCM, rt, 78 h, 94%; (d) *N*-succinimidyl *N*-methyl carbamate, DIPEA, DCM, rt, 9 h, 97%.

4).[60] Derivatives of **12** and **13** would then allow us to easily attach the *N*-methylcarbamoylguanidino moiety to the hydroxyl group at the C3, C5, or C9 position of the aglycone, using azide **14** and pyrazole carboxamidine **15**, in order to determine the appropriate position which will influence or determine their biological activities.

Furthermore, we envisioned that the amino sugar of **1**, desosamine, which is responsible for bestowing antibacterial properties, would best be removed, leading to chitinase inhibitors without any antibacterial property. We began by investigating appropriate positions and linkers to introduce the *N*-methylcarbamoylguanidino moiety via a triazole linker through copper-catalyzed triazole formation and a carbamate linker. The preparation method of azide **14** and pyrazole carboxamidine **15** is depicted in Scheme 1. Treatment of 2-bromoethylamine hydrobromide (**16**) with NaN_3 afforded the corresponding 2-azide ethylamine (not shown), followed by guanidine formation with *N*,*N*′-di-Boc-1*H*-pyrazole-1-carboxamidine to produce **17** in 94% yield over two steps. Carbamate formation with *N*-methyl-*p*-methoxybenzylamine generated **18** (91% yield)[61] and was followed by deprotection under acidic conditions to produce **14** in 94% yield as a free salt, leading to a triazole linkage. Urea formation with *N*-succinimidyl *N*-methyl carbamate of 1*H*-pyrazole-1-carboxamidine hydrochloride (**19**) afforded a 97% yield of pyrazole carboxamidine **15**, which potentially reacts with amine moieties, leading to a carbamate linkage (Scheme 1).

To form a triazole linker at the C9 position, treatment of **12** with propargyl bromide afforded **20** (41% yield), with subsequent copper-catalyzed triazole formation[62,63] with **14** to produce **21** in 40% yield (from **20**). To form triazole linkers at the C3 and C5 positions, treatment of **13** with propargyl bromide and NaH afforded both 5-*O*-propargyl **22** and 3-*O*-propargyl derivative **23** in 32% and 41% yields, respectively, with no dipropargyl byproduct. Copper-catalyzed triazole formation of **14** with **22** or **23** produced **24** or **27** in 61% and 69% yields, respectively, introducing the *N*-methylcarbamoylguanidino moiety (Scheme 2). To form a carbamate linker at the C3 position, we designed a derivative **26** including a carbamate linker with the same lengths as triazole **24** and **27**. Treatment of **22** with 1,1′-carbonyldiimidazole (CDI) generated **25** in 88% yield. Addition of 1,4-diaminobutane provided the precursor, which was subjected to conditions of *N*-methylcarbamoylguanidino formation with **15** to afford **26** in 61% yield. Conversely, to form a carbamate linker at the C5 position, **23** could not form the desired carbamate **28** because of undesirable cyclic carbonate formation at the C5 and C6 positions.

The IC_{50} values of tested compounds are shown in Table 1, specifically, **26** (0.217 μM) < **27** (3.3 μM) < **24** (11.9 μM) < **21** (24.1 μM). These data indicate that introduction of a pharmacophore at the C3 position still allows for interaction with *Sm*ChiB, even with the existence of a 14-membered macrolide, which might cause steric hindrance. Consequently, we began to synthesize focused derivatives (**29**−**32**) via carbamate linkers with different carbon lengths at the C3 position (Scheme 3). We envisioned that the propargyl group could be utilized for chemoselective introduction of a carbamate group using CDI. Treatment of **25** with various bis-amines possessing different carbon lengths provided the precursors, which were subjected to conditions for *N*-methylcarbamoylguanidino formation with **15** to afford **29**−**32** in 22−40% yields over two steps. Fortunately, **30** (n = 3, 0.036 μM, Table 2) was found to possess chitinase inhibition against *Sm*ChiB[37] almost 200 times more potent than that of **10** (6.4 μM). The clogP of **30** (clogP = 1.14) increased to a more suitable range than that of **10**. As expected, no chitinase inhibition was observed for **1** and the building blocks **13**, **15**, and **22** (>300 μM). Additionally, the truncated analog **14** showed only IC_{50} = 7.0 μM, almost the same as **10** (6.4 μM). This means the *N*-methylcarbamoylguanidino group is a pharmacophore, which can be regarded as a minimum functional group for generating chitinase inhibitory activity against *Sm*ChiB. These results clearly suggest that combination of the *N*-methylcarbamoylguanidino group and the macrolide aglycone participates in production of the potent nanomolar inhibition of *Sm*ChiB. In contrast, the inhibition of *Sm*ChiB of **29** (n = 2, 8.3 μM) decreased compared with that of **10**, while **26** (n = 4, 0.217 μM) and **31** (n = 5, 0.374 μM) showed activity 10 times less potent than that of **30** (0.036 μM). The analog **32**

DOI: 10.1021/acs.jmedchem.5b00175
J. Med. Chem. XXXX, XXX, XXX−XXX

Scheme 2. Synthesis of Derivatives with an *N*-Methylcarbamoylguanidino Group at C3, 5, and 9 Positions[a]

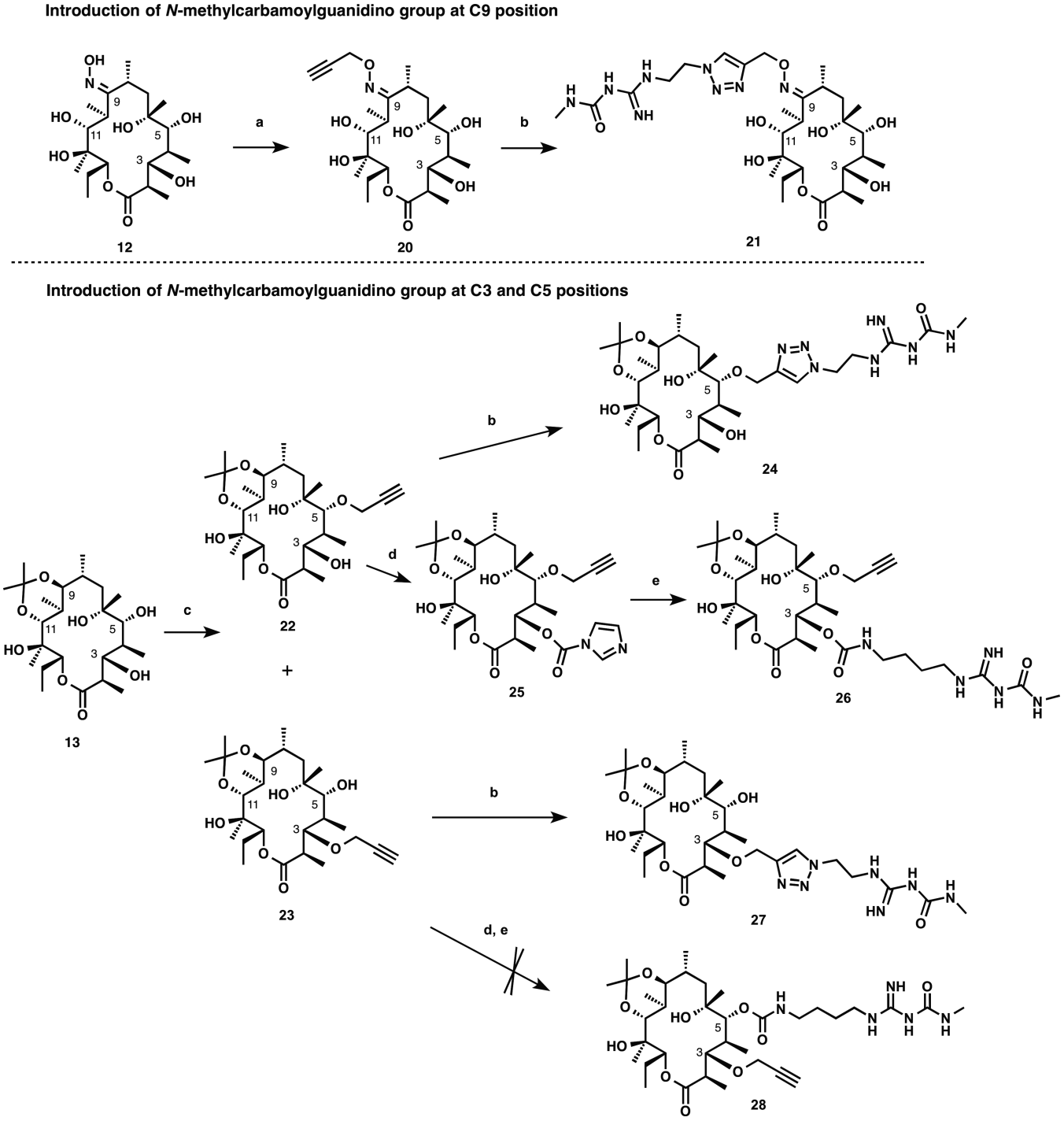

[a]Reagents and conditions: (a) propargyl bromide, K_2CO_3, DMF, rt, 41%; (b) **14**, $Cu(PF_6)(MeCN)$, TBTA, MeOH, rt, 40% (**21**), 61% (**24**), 69% (**27**); (c) propargyl bromide, NaH, TBAI, THF, rt, 3 h, 32% (**22**), 41% (**23**); (d) CDI, NaH, THF, rt, 88%, (e) (1) $NH_2(CH_2)_4NH_2$, THF, rt, 3 h, (2) **15**, DIPEA, THF, 55 °C, 61% over 2 steps.

(n = 7, 1.7 μM) exhibited an activity approximately 50 times lower than that of **30**. We were intrigued as to what role the isopropylidene acetal group of **30** plays. Thus, removal of the isopropylidene acetal group of **30** under acidic conditions provided the diol **33** in 44% yield. As a result, the *Sm*ChiB inhibition of **33** (1.4 μM) decreased, indicating that the isopropylidene acetal group may interact hydrophobically with *Sm*ChiB.

It is worth noting that **30** did not show any antibacterial activity (MIC > 64 μg/mL, Table 3)[64] against 27 types of bacteria, including Gram-positive and -negative bacteria. This result indicates that any undesirable antibacterial activity can be removed through molecular design.

Binding Modes of Macrolides with *Sm*ChiB. Given these results, we focused on understanding how *Sm*ChiB recognizes **26** and **29**−**33** at the atomic level and determined the crystal structures of **26** and **29**−**33** at 2.0−2.6 Å resolution

DOI: 10.1021/acs.jmedchem.5b00175
J. Med. Chem. XXXX, XXX, XXX−XXX

Table 1. Chitinase Inhibitory Activity of Argifin (10) and Derivative Compounds (21, 24, 26, and 27)

compd	IC_{50} (μM)[a]
argifin (**10**)	6.4
21	24.1
24	11.9
26	0.217
27	3.3

[a]Against *Sm*ChiB.

Scheme 3. Synthesis of Macrolide Derivatives 29−33 with a Aarbamate Linker[a]

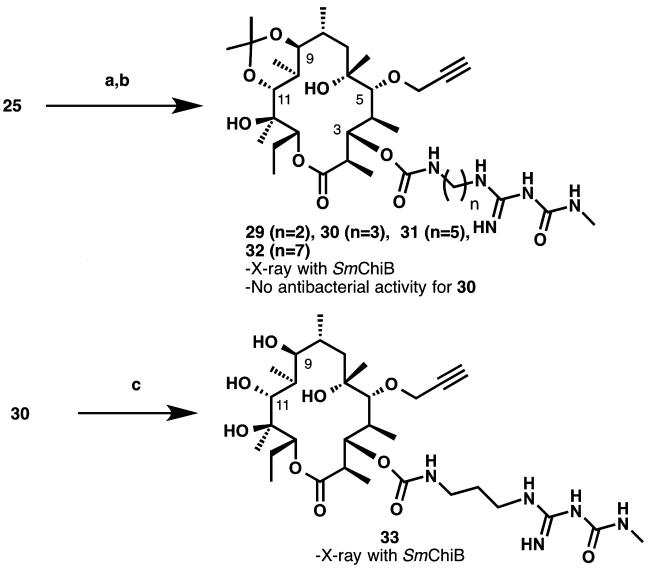

[a]Reagents and conditions: (a) bis-amines ($NH_2(CH_2)_2NH_2$, $NH_2(CH_2)_3NH_2$, $NH_2(CH_2)_5NH_2$, $NH_2(CH_2)_7NH_2$), THF, rt, 2−3 h; (b) **15**, DIPEA, THF, 55 °C, 39% (**29**), 33% (**30**), 34% (**31**), 22% (**32**) over 2 steps; (c) 90% AcOH aq, 100 °C, 44%.

Table 2. *Sm*ChiB Inhibition of 4, 10, 13−15, 22, 26, and 29−33

compd	IC_{50} (μM)[a]	compd	IC_{50} (μM)[a]
allosamidin (**4**)	0.09	**29** (n = 2)	8.3
argifin (**10**)	6.4	**30** (n = 3)	0.036
13	>300	**26** (n = 4)	0.217
14	7.0	**31** (n = 5)	0.374
15	>300	**32** (n = 7)	1.7
22	>300	**33**	1.4

[a]Against *Sm*ChiB.

after soaking.[53] The structures revealed that all inhibitors (**26** and **29−33**) were bound at the catalytic center (Asp142, Glu144, and Tyr214) through the *N*-methylcarbamoylguanidino group (Figure 5A) via the same binding mode as **10** (Figure 5B). Therefore, our strategy for creating an inhibitor design was validated. In addition, we unexpectedly observed another inhibitor bound to the substrate binding clefts in **26** (n = 4), **30** (n = 3), and **31** (n = 5), indicating that there are two potential binding sites (sites 1 and 2) at the substrate binding cleft of *Sm*ChiB (Figure 5A). A major binding site (site 1) is located above the catalytic center, which corresponds to the −2 position of the chitin substrate (Figure 5A) and overlaps with the allosamidin (**4**) binding site in subsite −2 to −1 (Figure 5D).[65] A minor site (site 2) is located opposite site 1, which corresponds to the +2 and +3 positions of $GlcNAc_5$ (Figure 5C). To the best of our knowledge, no molecules have been reported that bind to site 2 in *Sm*ChiB, indicating that a new binding position on a family-18 chitinase was observed. As predicted by the *B*-factor of inhibitors, binding to site 2 was not as strong as binding to site 1. Site 2 binding mainly involved hydrophobic (Trp97, Phe190, Phe191, Trp220, Phe239, and Glu221) interactions with the *N*-methylcarbamoylguanidino group. The inhibitors at site 2 formed a compact, bent conformation (Figure 5E). The *B*-factor of the inhibitors in site 2 was higher than that in site 1. The molecular mechanics (MM) interaction energy[66] of inhibitors using site 2 (−124.73 kcal/mol for **30**) was much less stable than that using site 1 (−172.29 kcal/mol for **30**). In addition, the MM energy of the bound conformation of **30** using site 2 (−103.97 kcal/mol) was much higher than that of **30** using site 1 (−113.87 kcal/mol), suggesting that site 2 binding requires a higher strain energy. Therefore, we determined that binding at site 2 would not be as strong as that at site 1 and that the binding mode using site 1 would be the main contributor to the binding affinities for **26**, **30**, and **31**. In **29** (n = 2), no electron density was observed at site 2, presumably because the alkyl linker length was too short to achieve the bent conformation. Compound **32** (n = 7) was bound to the catalytic center through the *N*-methylcarbamoylguanidino group and to site 2 with the macrolide moiety;

Table 3. MIC Values for Antibacterial Activity of 30

entry	strain/compd	MIC (μg/mL) of **30**
1	*Staphylococcus aureus* FDA209P[a]	>64
2	*Staphylococcus aureus* Smith[a]	>64
3	*Staphylococcus aureus* KUB853[b]	>64
4	*Staphylococcus aureus* KUB854[b]	>64
5	*Staphylococcus aureus* 70[b]	>64
6	*Staphylococcus aureus* 92-1191[b]	>64
7	*Staphylococcus aureus* KUB857[c]	>64
8	*Staphylococcus aureus* KUB858[d]	>64
9	*Staphylococcus aureus* Mu50[b,e]	>64
10	*Staphylococcus aureus* KUB877[b,f]	>64
11	*Staphylococcus epidermidis* KUB795	>64
12	*Micrococcus luteus* ATCC9341	>64
13	*Enterococcus faecalis* ATCC29212	>64
14	*Enterococcus faecalis* NCTC12201(VanA)[g]	>64
15	*Enterococcus faecium* NCTC12204(VanA)[g]	>64
16	*Escherichia coli* NIHJ JC-2	>64
17	*Citrobacter freundii* ATCC8090	>64
18	*Klebsiella pneumoniae* NCTC9632	>64
19	*Proteus mirabilis* IFO3849	>64
20	*Proteus vulgaris* OX-19	>64
21	*Morganella morganii* IID Kono	>64
22	*Serratia marcescens* IFO12648	>64
23	*Enterobacter cloacae* IFO13535	>64
24	*Enterobacter aerogenes* NCTC10006	>64
25	*Pseudomonas aeruginosa* 46001	>64
26	*Pseudomonas aeruginosa* E-2	>64
27	*Acinetobacter calcoaceticus* IFO12552	>64

[a]MSSA: methicillin-sensitive *Staphylococcus aureus*. [b]MRSA: methicillin-resistant *Staphylococcus aureus*. [c]Macrolide-resistant *Staphylococcus aureus* strain that has inducible *erm* genes. [d]Macrolide-resistant *Staphylococcus aureus* strain that constitutively expresses *erm* genes. [e]VISA: vancomycin-intermediate *Staphylococcus aureus*. [f]Linezolid resistance. [g]VRE: vancomycin-resistant *Enterococci*.

DOI: 10.1021/acs.jmedchem.5b00175
J. Med. Chem. XXXX, XXX, XXX−XXX

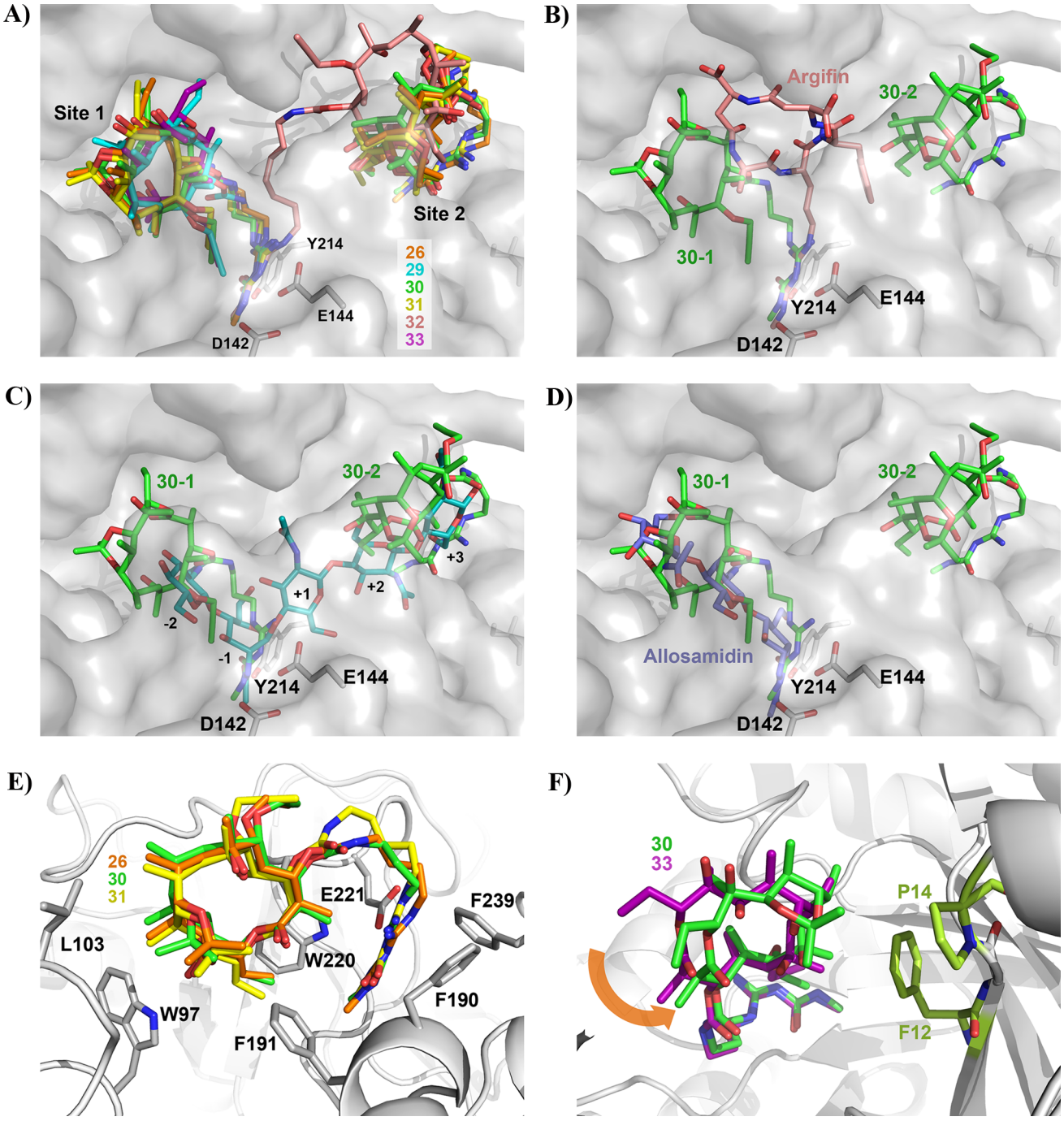

Figure 5. X-ray analysis of *Sm*ChiB with designed 14-membered macrolides. (A) The substrate binding cleft of *Sm*ChiB structure is complexed with inhibitors. The catalytic residues D142, E144, and Y214 are also shown: **26** (orange), **29** (light blue), **30** (green), **31** (yellow), **32** (pink), **33** (magenta). (B) Superposed model of **30** (green) and **10** (pink). (C) Superposed model of **30** (green) and $GlcNAc_5$ (blue). (D) Superposed model of **30** (green) and allosamidin (**4**, purple). (E) Close-up view of site 2 with **26** (orange), **30** (green), and **31** (yellow). (F) Comparison of **30** (green) and **33** (magenta). The arrow indicates that **30** is moved close to the hydrophobic site composed of Pro14 and Phe12.

however, no electron density from the macrolide **32** at site 1 was observed. Macrolide binding at sites 1 and 2 varies according to the length of the alkyl linker. Namely, when the chain length was between 2 and 5, the inhibitor could bind to both the catalytic center and site 1 in a single molecule, whereas when chain length was longer than 7, the macrolide portion could not bind at site 1, only at site 2. The IC_{50} values indicate that macrolide binding at site 1 enhances the binding affinity, presumably because of site 1 being better fitted to the macrolide structure than site 2. These results suggest that inhibitor binding at the catalytic center with the *N*-methylcarbamoylguanidino group is essential and macrolide binding at site 1 strengthens the inhibitor binding. We observed that the customized macrolides were located in the same place as allosamidin (**4**) when the main scaffold was replaced with the macrocyclic configuration from a cyclic peptide. This observation indicates that the macrocyclic configuration possibly mimics a carbohydrate cluster. In comparing **30** and **33**, we found that **33** was located away from the hydrophobic moieties (Phe12 and Pro14, Figure 5F), indicating that the

DOI: 10.1021/acs.jmedchem.5b00175
J. Med. Chem. XXXX, XXX, XXX−XXX

Table 4. Results of Binding Free Energy Analysis Using the MM-PBSA Method

compd	IC_{50}, μM	free energy, kcal/mol				
		ΔG_{bind}	$\Delta G_{bind(bound\ form)}$	$\Delta G_{adapt(protein)}$	$\Delta G_{adapt(ligand)}$	$\Delta G_{adapt(protein)} + \Delta G_{adapt(ligand)}$
29 (n = 2)	8.3	−22.63	−47.71	20.41	4.67	25.08
30 (n = 3)	0.036	−29.04	−45.62	18.08	−1.50	16.58
26 (n = 4)	0.217	−26.65	−48.62	21.90	0.07	21.98
31 (n = 5)	0.374	−26.34	−42.81	13.34	3.13	16.47

isopropylidene acetal group of **30** participates in hydrophobic interactions.

Computed Analysis. To explore the cause of dependence of the inhibitory activity on the linker length, we performed binding free energy analyses of **26** and **29**−**31** in site 1 of *Sm*ChiB using the molecular mechanics Poisson−Boltzmann surface area (MM-PBSA) method combined with a molecular dynamics (MD) simulation.[53]

We used the three-trajectory approach, in which separate trajectories of the complex, protein, and ligand were performed to calculate their free energies ($G_{complex}$, $G_{protein(free)}$, and $G_{ligand(free)}$, respectively). The binding free energy (ΔG_{bind}) was also estimated according to eq 1 below.

$$\Delta G_{bind} = G_{comples} - G_{portein(free)} - G_{ligand(free)} \quad (1)$$

This approach also allows us to discuss the free energy costs of the conformational adaptation upon binding of proteins and ligands, as eq 1 can be transformed into eq 2.

$$\Delta G_{bind} = \Delta G_{bind(bound\ form)} + \Delta G_{adapt(protein)} + \Delta G_{adapt(ligand)} \quad (2)$$

The value of $\Delta G_{bind(bound\ form)}$ was given by ($G_{complex} - G_{protein(bound)} - G_{ligand(bound)}$). The values of $G_{protein(bound)}$ and $G_{ligand(bound)}$ were estimated using their bound structures in the MD trajectories of the complex. The values of $\Delta G_{adapt(protein)}$ and $\Delta G_{adapt(ligand)}$ were calculated as ($G_{protein(bound)} - G_{protein(free)}$) and ($G_{ligand(bound)} - G_{ligand(free)}$), respectively.

We identified a strong correlation between ΔG_{bind} values and the experimental IC_{50} values (Table 4). We also found that consideration of the conformational adaptation was important for quantitative analysis in this study, as $\Delta G_{bind(bound\ form)}$ showed low correlation with the experimental values. The sum of $\Delta G_{adapt(protein)}$ and $\Delta G_{adapt(ligand)}$ for **29** (n = 2) was the highest among the compounds, suggesting that the binding of **29** with *Sm*ChiB requires the largest conformational strain. This energy cost seems to cause ΔG_{bind} of **29** to be the weakest. This result is in agreement with the experimental value, indicating that **29** possesses the weakest IC_{50} value. Conversely, **30** (n = 3) showed a relatively low $\Delta G_{adapt(protein)}$ and the smallest $\Delta G_{adapt(ligand)}$ among the compounds. The $\Delta G_{adapt(ligand)}$ for **30** was a negative value near zero, suggesting that **30** does not experience conformational strain upon binding to *Sm*ChiB. Therefore, the sum of $\Delta G_{adapt(protein)}$ and $\Delta G_{adapt(ligand)}$ for **30** was much lower than those for **26** (n = 4) and **29**. As a result, ΔG_{bind} for **30** was estimated to be greater than those for **26** and **29**. Although **31** (n = 5) showed a sum of $\Delta G_{adapt(protein)}$ and $\Delta G_{adapt(ligand)}$ similar to that of **30**, its $\Delta G_{bind(bound\ form)}$ was weaker than that of **30**. Therefore, ΔG_{bind} for **30** was estimated to be greater than that for **31**. On the basis of these observations, we determined that the linear length of **30** was the most appropriate for binding to site 1 of *Sm*ChiB, from an energy perspective.

CONCLUSIONS

We designed and synthesized a novel and potent chitinase inhibitor (**30**) using a macrolide scaffold that holds promise for development of a customized new class of chitinase inhibitors with a novel skeleton and no undesirable antibiotic characteristics. Moreover, from X-ray crystallography and the energy point obtained computationally, we revealed the binding modes of six macrolides with *Sm*ChiB and relevant structures, indicating why **30** shows inhibition that is an order of magnitude stronger than that of **10**. Interestingly, **30** was found to mimic **4**, with respect to the binding site. This result suggests that the macrocyclic motif may be able to mimic a carbohydrate cluster. Overall, this study offers insight for drug design, confirms the potential of using macrolides as flexible templates for drug discovery, and delivers potential for the creation of a new class of chitinase inhibitors boasting novel skeletal structures. A pharmacokinetic study of customized macrolide inhibitors and investigations of the applications of this approach in various natural products are currently underway.

EXPERIMENTAL SECTION

Chemistry. General Methods. All reagents were used as purchased without further purification unless otherwise noted. Unless otherwise noted, all reactions were carried out under nitrogen atmosphere. Precoated silica gel plates with a fluorescent indicator (Merck Ltd., Tokyo, Japan, 60 F254) were used for analytical and preparative thin layer chromatography. Flash column chromatography was carried out with Kanto Chemical silica gel (Kanto Chemical Co., Inc., Tokyo, Japan, Silica gel 60N, spherical neutral, 0.040−0.050 mm, catalog no. 37563-84) or Merck silica gel 230−400 mesh ASTM (Merck Ltd., Tokyo, Japan, 60N, 0.040−0.063 mm, catalog no. 109385). ^{1}H NMR spectra were recorded at 500 MHz, and ^{13}C NMR spectra were recorded at 125 MHz on JEOL ECA-500 (500 MHz) (JEOL Ltd., Tokyo, Japan). The chemical shifts are expressed in ppm downfield from internal solvent peaks $CDCl_3$ (7.26 ppm, ^{1}H NMR), CD_3OD (3.31, 4.84 ppm, ^{1}H NMR), $CDCl_3$ (77.0 ppm, ^{13}C NMR), CD_3OD (49.0 ppm, ^{13}C NMR), and J values are given in hertz. The coupling patterns are expressed by s (singlet), d (doublet), dd (double doublet), ddd (double double doublet), dt (double triplet), t (triplet), m (multiplet), or br (broad). All infrared spectra were measured on a Horiba FT-210 spectrometer (HORIBA Ltd., Kyoto, Japan). High- and low-resolution mass spectra were measured on a JEOL JMS-700 MStation and JEOL JMS-T100LP (JEOL Ltd., Tokyo, Japan). Melting points were measured on a Yanaco micro melting system MP-500P (Yanaco New Science Inc., Kyoto, Japan).

Method A. HPLC analysis was performed on a Waters 2795 separation module with Alliance HT (Nihon Waters K. K., Tokyo, Japan) equipped with a diode-array detector and micromass ZQ (Nihon Waters K. K., Tokyo, Japan) (column, Senshu Pak-PEGASIL ODS SP100 2 ⌀ × 50 mm (Senshu Scientific Co., Ltd., Tokyo, Japan)). Condition of HPLC: gradient 10% MeCN (0.05% TFA)/H_2O (0.1% TFA) to 100% MeCN (0.05% TFA) over 8 min, flow 0.3 mL/min, detect 210−400 nm, temperature 20 °C.

Method B. HPLC analysis was performed on a model LaChrom Elite system (Hitachi High-Tech Science Co., Tokyo, Japan) equipped with a diode-array detector (column, Inertsil ODS-4 (3.0 ⌀ × 250 mm,

DOI: 10.1021/acs.jmedchem.5b00175
J. Med. Chem. XXXX, XXX, XXX−XXX

GL Sciences, Tokyo, Japan). Condition of HPLC: gradient 5% MeCN/H_2O (0.1% HCOOH) to 100% MeCN over 30 min, flow 0.5 mL/min, detect 210 nm, temperature 40 °C.

Method C. HPLC analysis was performed on a model LaChrom Elite system (Hitachi High-Tech Science Co., Tokyo, Japan) equipped with a 3300 ELSD detector (Astech Inc., Tokyo, Japan) (column, PEGASIL ODS SP100 (4.6 ⌀ × 250 mm, Senshu Scientific Co., Ltd., Tokyo, Japan). Condition of HPLC: isocratic 60% MeCN/H_2O over 20 min, flow 1.0 mL/min, temperature 24 °C.

{*N*,*N*′-Bis(*tert*-butoxycarbonyl)-*N*″-2-azidoethyl}guanidine: 17. To a solution of 2-Bromoethylamine hydrobromide (**16**) (70.0 mg, 0.341 mmol) in H_2O (0.34 mL) was added NaN_3 (66.6 mg, 1.025 mmol) at room temperature. The reaction mixture was heated to reflux and stirred for 5 h. After being cooled to room temperature, to the mixture were added MeCN (2 mL), *N*,*N*′-di-Boc-1*H*-pyrazole-1-carboxamidine (116 mg, 0.376 mmol), and DIPEA (734 μL, 4.10 mmol). The mixture was stirred at room temperature for 15 h and quenched with saturated aqueous NH_4Cl (10 mL), extracted with $CHCl_3$ (10 mL × 4). The combined organic layers were dried over Na_2SO_4 and concentrated in vacuo. The crude product was purified by flash column chromatography (hexanes/EtOAc = 20/1 to 7/1) to afford **17** (106 mg, 0.323 mmol, 94% over 2 steps) as a colorless solid. Mp 76−78 °C. IR (KBr) ν cm^{-1}: 3332, 2978, 2931, 2103, 1741, 1626, 1367, 1223, 1146, 1113, 1057, 864, 818, 762. ^1H NMR (500 MHz, CD_3OD) δ (ppm): 3.55, 3.49, 1.53, 1.47. ^{13}C NMR (125 MHz, CD_3OD) δ (ppm): 164.4, 157.8, 154.0, 84.6, 80.5, 51.2, 41.0, 28.9, 28.2. HRMS (FAB, NBA) *m*/*z*: 329.1937 $[M + H]^+$; calcd for $C_{13}H_{25}N_6O_4$, 329.1937. HPLC analysis (method A): retention time = 6.90 min; peak area, >99%.

{*N*-(*N*′-*p*-Methoxybenzyl-*N*′-methylcarbamoyl)-*N*″-(*tert*-butoxycarbonyl)-*N*‴-2-azidoethyl}guanidine: 18. To a solution of compound **17** (67.5 mg, 0.206 mmol) in THF (4 mL) was added *N*-methyl-*p*-methoxybenzylamine (40.4 mg, 0.267 mmol). The reaction mixture was heated to reflux and stirred for 16 h. After being cooled to room temperature, the solvent was removed in vacuo. The residue was purified by flash column chromatography (hexanes/EtOAc = 10/1 to 7/1) to afford **18** (76.2 mg, 0.188 mmol, 91%) as a colorless oil. IR (KBr) ν cm^{-1}: 3334, 2979, 2935, 2100, 1718, 1633, 1595, 1512, 1389, 1321, 1244, 1151, 1032. ^1H NMR (500 MHz, CD_3OD) δ (ppm): 7.18−7.13 (complex m, 2H, rotamer), [6.870 (d, *J* = 8.6 Hz, rotamer), 6.866 (d, *J* = 8.6 Hz, rotamer)], [4.70, 4.45 (s × 2, 2H, rotamer), [3.764, 3.760 (s × 2, 3H, rotamer)], [3.59−3.33 (complex m, 4H, rotamer)], [2.99, 2.84 (s × 2, 3H, rotamer)], [1.514, 1.509 (s × 2, 9H, rotamer)]. ^{13}C NMR (125 MHz, CD_3OD) δ (ppm): [165.6, 165.4 (rotamer)], [160.40, 160.35 (rotamer)], [155.4, 155.3 (rotamer)], [154.24, 154.18 (rotamer)], [131.8, 131.4 (rotamer)], [130.0, 129.3 (rotamer)], [114.98, 114.94 (rotamer)], 83.9, 55.7, [53.5, 51.2 (rotamer)], [51.12, 51.06 (rotamer)], 41.1, [35.2, 33.5, rotamer], [28.3, 28.2, rotamer]. HRMS (FAB, NBA) *m*/*z*: 428.2021 $[M + Na]^+$; calcd for $C_{18}H_{27}N_7NaO_4$, 428.2022. HPLC analysis (method A): retention time = 7.70 min; peak area, 97%.

(*N*-Methylcarbamoyl-*N*′-azidoethyl)guanidine: 14. The starting material **18** (39.0 mg, 0.0962 mmol) was dissolved in 90%TFA/DCM (2 mL). The reaction was stirred for 7 h. After removal of the solvent in vacuo, the residue was purified by flash column chromatography ($CHCl_3$/MeOH/NH_4OH = 20/1/0.1 to 10/1/0.1) to afford **14** (16.8 mg, 0.0907 mmol, 94%) as a colorless oil. IR (KBr) ν cm^{-1}: 3332, 2438, 2098, 1550, 1435, 1389, 1296. ^1H NMR (500 MHz, CD_3OD) δ (ppm): 3.42 (m, 2H), 3.35 (m, 2H), 2.68 (s, 3H). ^{13}C NMR (125 MHz, CD_3OD) δ (ppm): 167.8, 161.3, 51.9, 41.1, 26.8. HRMS (FAB, NBA) *m*/*z*: 186.1103 $[M + H]^+$; calcd for $C_5H_{12}N_7O$, 186.1103. HPLC analysis (method A): retention time = 0.67 min; peak area, >99%.

***N*′-(*N*-Methylcarbamoyl)-1*H*-pyrazole-1-carboxamidine: 15.** To a solution of 1*H*-pyrazole-1-carboxamidine hydrochloride (**19**) (926 mg, 6.32 mmol) in DCM (57.0 mL) were added *N*-succinimidyl *N*-methyl carbamate (1.00 g, 5.74 mmol) and DIPEA (2.20 mL, 12.6 mmol). The mixture was stirred at room temperature for 9 h under N_2. After the solvent was removed in vacuo, the residue was purified by flash column chromatography (only $CHCl_3$) to afford **15** (935 mg, 5.59 mmol, 97%) as a colorless solid. Mp 109−113 °C. IR (KBr) ν cm^{-1}: 3390, 3330, 3222, 1647, 1504, 1398, 1300, 1190, 1031, 955. ^1H NMR (500 MHz, CD_3OD) δ (ppm): 8.39 (d, *J* = 2.9 Hz, 1H), 7.71 (s, 1H), 6.44 (dd, *J* = 2.6, 1.4 Hz, 1H), 2.76 (s, 3H). Note: The rotamers were observed as minor peaks. ^{13}C NMR (125 MHz, CD_3OD) δ (ppm): 166.9, 153.7, 144.0, 129.3, 109.5, 26.9. Note: The rotamers were observed as minor peaks. HRMS (FAB, PEG600) *m*/*z*: 168.0883 $[M + H]^+$; calcd for $C_6H_9N_5O$, 168.0885. HPLC analysis (method A): retention time = 1.02 min; peak area, >99%.

Erythronolide A *O*-Propargyloxime: 20. To a solution of **12** (100 mg, 0.231 mmol) in DMF (2.3 mL) were added K_2CO_3 (115.5 mg, 1.15 mmol) and propargyl bromide (0.10 mL, 1.15 mmol). The reaction mixture was stirred at room temperature for 6 h. To the mixture was added sat. NH_4Cl aq (10 mL × 1) followed by extraction with EtOAc (10 mL) and washing with brine (10 mL × 5). The organic layer was dried over Na_2SO_4, filtered and concentrated in vacuo. The crude product was purified by flash column chromatography ($CHCl_3$/MeOH = 50/1 to 30/1) to afford **20** (45.0 mg, 0.0954 mmol, 41%) as a yellow solid. Mp 181−183 °C. $[\alpha]^{28}_D$ −28.5 (*c* 1.0, MeOH). IR (KBr) ν cm^{-1}: 3589, 3483, 3269, 2968, 2879, 1720, 1460, 1377, 1350, 1288, 1263, 1184, 1082, 1032, 1002, 958. ^1H NMR (500 MHz, CD_3OD) δ (ppm): 5.32 (dd, *J* = 11.5, 2.3 Hz, 1H), 4.63 (d, *J* = 2.3 Hz, 2H), 3.79 (d, *J* = 1.2 Hz, 1H), 3.68 (dq, *J* = 16.3, 6.9 Hz, 1H), 3.47 (d, *J* = 10.9 Hz, 1H), 3.39 (d, *J* = 3.4 Hz, 1H), 2.86 (t, *J* = 2.6 Hz, 1H), 2.78 (q, *J* = 6.9 Hz, 1H), 2.67 (dq, *J* = 10.3, 6.9 Hz, 1H), 2.09−2.01 (m, 1H), 1.97−1.87 (m, 1H), 1.61 (dd, *J* = 14.3, 11.5 Hz, 1H), 1.55−1.44 (m, 1H), 1.38−1.33 (m, 1H), 1.34 (s, 3H), 1.20 (d, *J* = 6.9 Hz, 3H), 1.18 (s, 3H), 1.17 (d, *J* = 6.9 Hz, 3H), 1.05 (d, *J* = 7.5 Hz, 3H), 0.94 (d, *J* = 7.5 Hz, 3H), 0.84 (t, *J* = 7.5 Hz, 3H). ^{13}C NMR (125 MHz, CD_3OD) δ (ppm): 177.0, 173.6, 82.0, 80.7, 79.6, 78.2, 76.1, 76.0, 75.8, 71.9, 61.9, 45.2, 37.6, 34.8, 27.9, 26.6, 22.6, 19.1, 17.4, 15.8, 15.3, 11.0, 8.4. HRMS (ESI^+) *m*/*z*: 494.2719 $[M + Na]^+$; calcd for $C_{24}H_{41}NNaO_8$, 494.2730. HPLC analysis (method A): retention time = 5.80 min; peak area, 97%.

Erythronolide A *O*-((1-(2-(*N*-Methylcarbamoylguanidino)-ethyl)-1*H*-1,2,3-triazol-4-yl)methyl)oxime: 21. To a solution of **20** (30.0 mg, 0.0636 mmol) in MeOH (0.6 mL) were added $Cu(PF_6)(MeCN)_4$ (2.4 mg, 0.00636 mmol) and TBTA (3,4 mg, 0.00636 mmol) and (*N*-methylcarbamoyl-*N*′-azidoethyl)guanidine **14** (13.0 mg, 0.0699 mmol). The reaction mixture was stirred at room temperature for 1 h. To the mixture were added saturated aqueous Rochelle salt (2 mL) and H_2O (1 mL). The resulting mixture was extracted with $CHCl_3$ (5 mL × 3), then the organic layer was dried over Na_2SO_4 and concentrated in vacuo. The crude product was purified by flash column chromatography ($CHCl_3$/MeOH/30% NH_4OH = 50/1/0.1 to 30/1/0.1) to afford **21** (16.5 mg, 0.025 mmol, 40%) as a colorless solid. Mp 122−126 °C. $[\alpha]^{23}_D$ −77.0 (*c* 0.84, MeOH). IR (KBr) ν cm^{-1}: 3398, 2976, 2939, 1722, 1618, 1514, 1458, 1375, 1219, 1173, 1082, 1038, 985, 758. ^1H NMR (500 MHz, CD_3OD) δ (ppm): 7.90 (s, 1H), 5.16−5.12 (complex m, 3H), 4.64 (m, 1H), 4.58 (m, 1H), 3.81 (m, 1H), 3.74 (m, 1H), 3.68−3.64 (complex m, 2H), 3.47 (d, *J* = 10.3 Hz, 1H), 3.39 (d, *J* = 3.4 Hz, 1H), 2.76 (m, 1H), 2.70 (s, 3H), 2.65 (m, 1H), 1.99 (m, 1H), 1.86 (m, 1H), 1.58 (dd, *J* = 14.3, 11.5 Hz, 1H), 1.46 (m, 1H), 1.36 (s, 3H), 1.33−1.27 (m, 1H), 1.17 (d, *J* = 6.9 Hz, 3H), 1.16 (s, 6H), 1.04 (d, *J* = 7.5 Hz, 3H), 0.93 (d, *J* = 7.5 Hz, 3H), 0.79 (t, *J* = 7.2 Hz, 3H). ^{13}C NMR (125 Hz, CD_3OD) δ (ppm): 176.9, 172.8, 167.7, 160.5, 146.5, 125.6, 82.0, 79.6, 78.2, 76.1, 75.6, 72.5, 67.4, 50.9, 45.2, 42.0, 37.6, 37.4, 34.5, 27.9, 26.8, 26.5, 22.5, 19.2, 17.5, 15.9, 15.5, 11.0, 8.4. HRMS (ESI^+) *m*/*z*: 679.3751 $[M + Na]^+$; calcd for $C_{29}H_{52}NNaO_9$, 679.3755. HPLC analysis (method A): retention time = 4.52 min; peak area, 98%.

(9*S*)-9-Dihydro-9,11-*O*-isopropylidene-5-*O*-propargyl-erythronolide A (22) and (9*S*)-9-Dihydro-9,11-*O*-isopropylidene-3-*O*-propargylerythronolide A (23). To a solution of **13** (253.0 mg, 0.549 mmol) in THF (5.5 mL) was added NaH (65.9 mg, 2.75 mmol) in 0 °C under N_2 atmosphere. After being stirred at 0 °C for 20 min, to the reaction mixture were added propargyl bromide (0.24 mL, 2.75 mmol) and TBAI (20.3 mg, 0.0549 mmol) at room temperature. The mixture was diluted with EtOAc (15 mL × 1), washed with saturated aqueous NH_4Cl (15 mL × 2) and brine (15 mL

DOI: 10.1021/acs.jmedchem.5b00175
J. Med. Chem. XXXX, XXX, XXX−XXX

× 1). The organic layer was dried over Na_2SO_4 and concentrated in vacuo. The crude product was purified by flash column chromatography (only $CHCl_3$) to afford **22** (88.8 mg, 0.178 mmol, 32%) as a colorless solid and **23** (112.0 mg, 0.225 mmol, 41%) as a colorless solid.

22: Mp 198−205 °C. $[\alpha]_D^{26}$ +5.2 (*c* 1.0, MeOH). IR (KBr) ν cm^{-1}: 3545, 3489, 3381, 3249, 2983, 2962, 2931, 2885, 2854, 1724, 1460, 1381, 1335, 1259, 1219, 1169, 1086, 1032, 889, 800, 690. ^{1}H NMR (500 MHz, CD_3OD) δ (ppm) 5.90 (s, 1H), 5.23 (dd, *J* = 11.2, 2.6 Hz, 1H), 4.28 (dd, *J* = 15.5, 2.3 Hz, 1H), 4.22 (dd, *J* = 15.5, 2.3 Hz, 1H), 3.63 (app t, *J* = 2.9 Hz, 1H), 3.52 (d, *J* = 2.9 Hz, 1H), 3.47 (dd, *J* = 10.6, 1.5 Hz, 1H), 3.24 (d, *J* = 3.4 Hz, 1H), 2.73 (t, *J* = 2.3 Hz, 1H), 2.67 (m, 1H), 2.16 (m, 1H), 2.10 (m, 1H), 2.01 (m, 1H), 1.90 (m, 1H), 1.78 (dd, *J* = 15.5, 9.2 Hz, 1H), 1.51 (m, 1H), 1.49 (s, 3H), 1.42 (s, 3H), 1.28 (m, 1H), 1.26 (s, 3H), 1.22 (d, *J* = 6.9 Hz, 3H), 1.20 (d, *J* = 6.9 Hz, 3H), 1.19 (s, 3H), 0.98 (d, *J* = 7.5 Hz, 3H), 0.95 (d, *J* = 7.5 Hz, 3H), 0.83 (t, *J* = 7.5 Hz, 3H). ^{13}C NMR (125 MHz, CD_3OD) δ (ppm) 176.7, 103.0, 88.4, 81.7 (2C), 78.2, 77.7, 75.3, 75.0, 74.8, 71.6, 59.1, 45.6, 39.3, 35.6, 33.7, 31.9, 28.0, 26.6, 24.3, 22.6, 20.0, 16.90, 16.87, 16.2, 10.8, 8.5. HRMS (ESI$^+$): 521.3082 [M + Na]$^+$; calcd for $C_{27}H_{46}NaO_8$, 521.3090. HPLC analysis (method C): retention time = 25.4 min; peak area, 98%.

23: Mp 157−161 °C. $[\alpha]_D^{25}$ +48.8 (*c* 1.0, MeOH). IR (KBr) ν cm^{-1}: 3437, 2976, 2937, 1732, 1631, 1460, 1379, 1230, 1169, 1074, 1034, 924. ^{1}H NMR (500 MHz, CD_3OD) δ (ppm) 5.19 (dd, *J* = 11.5, 2.3 Hz, 1H), 4.41 (dd, *J* = 15.5, 2.3 Hz, 1H), 4.35 (dd, *J* = 15.5, 2.3 Hz, 1H), 3.67 (d, *J* = 9.8 Hz, 1H), 3.64 (dd, *J* = 2.9, 2.9 Hz, 1H), 3.57 (d, *J* = 3.5 Hz, 1H), 3.50 (d, *J* = 2.3 Hz, 1H), 2.87 (t, *J* = 2.3 Hz, 1H), 2.74 (dq, *J* = 10.3, 6.9 Hz, 1H), 2.17 (m, 1H), 1.99 (m, 1H), 1.96 (m, 1H), 1.89 (m, 1H), 1.74 (dd, *J* = 15.5, 8.6 Hz, 1H), 1.51 (m, 1H), 1.49 (s, 3H), 1.44 (s, 3H), 1.29 (d, *J* = 15.5 Hz, 1H), 1.26 (d, *J* = 6.9 Hz, 3H), 1.22 (s, 3H), 1.20 (d, *J* = 6.9 Hz, 3H), 1.17 (s, 3H), 0.99 (d, *J* = 6.9 Hz, 3H), 0.98 (d, *J* = 7.5 Hz, 3H), 0.83 (t, *J* = 7.5 Hz, 3H). ^{13}C NMR (125 MHz, CD_3OD) δ (ppm) 176.4, 103.0, 87.0, 81.7, 81.2, 81.0, 77.9, 76.00, 75.97, 75.0, 71.7, 60.4, 45.8, 39.0, 35.1, 33.9, 31.9, 28.0, 26.4, 24.3, 22.5, 19.9, 16.9 (2C), 16.3, 10.8, 9.2. HRMS (FAB, NBA): 499.3270 [M + H]$^+$; calcd for $C_{27}H_{47}O_8$, 499.3271. HPLC analysis (method C): retention time = 8.35 min; peak area, >99%.

(9*S*)-9-Dihydro-9,11-*O*-isopropylidene-5-*O*-((1-(2-(*N*-methylcarbamoylguanidino)ethyl)-1*H*-1,2,3-triazol-4-yl)-methyl)erythronolide A: 24. According to the preparation of **21**, **22** (20.0 mg, 0.0401 mmol) was converted to **24** (16.8 mg, 0.0246 mmol) in 61% yield as a colorless solid. Mp 115−118 °C. $[\alpha]_D^{25}$ −1.80 (*c* 1.0, MeOH). IR (KBr) ν cm^{-1}: 3319, 2970, 2937, 1732, 1616, 1514, 1458, 1377, 1227, 1165, 1086, 1032. ^{1}H NMR (500 MHz, CD_3OD) δ (ppm): 7.93 (s. 1H), 5.24 (dd, *J* = 11.5, 2.3 Hz, 1H), 4.82 (d, *J* = 12.0 Hz, 2H), 4.27−4.54 (m, 3H), 3.69 (brt, *J* = 5.7 Hz, 2H), 3.62 (t, *J* = 2.9 Hz, 1H), 3.55−3.50 (m, 2H), 3.20 (d, *J* = 2.9 Hz, 1H), 2.75−2.67 (m, 1H), 2.70 (s, 3H), 2.17−2.09 (m, 2H), 2.00 (m, 1H), 1.90 (m, 1H), 1.77 (m, 1H), 1.56−1.47 (m, 1H), 1.48 (s, 3H), 1.42 (s, 3H), 1.29 (m, 1H), 1.25 (d, *J* = 6.3 Hz, 3H), 1.20 (d, *J* = 4.5 Hz, 3H), 1.19 (s, 3H), 1.08 (s, 3H), 1.03 (d, *J* = 7.5 Hz, 3H), 0.95 (d, *J* = 6.9 Hz, 3H), 0.84 (t, *J* = 7.5 Hz, 3H). ^{13}C NMR (500 MHz, CD_3OD) δ (ppm): 176.8 167.2, 160.7, 146.2, 125.7, 103.0, 88.7, 81.7, 78.4, 77.8, 75.5, 75.0, 71.6, 64.9, 50.7, 45.6, 41.7, 39.4, 35.6, 33.7, 31.8, 28.0, 26.8, 26.5, 24.2, 22.6, 20.0, 16.9 (2C), 16.2, 10.8, 8.7. HRMS (ESI$^+$): 706.4106 [M + Na]$^+$; calcd for $C_{32}H_{57}N_7NaO_9$, 706.4115. HPLC analysis (method A): retention time = 5.08 min; peak area, 99%.

(9*S*)-9-Dihydro-3-imidazoylcarbonyl-9,11-*O*-isopropylidene-5-*O*-propargylerythronolide A: 25. To a solution of **22** (50.0 mg, 0.100 mmol) in THF (2 mL) were added NaH (21.9 mg, 0.50 mmol) and carbonyldiimidazole (81.3 mg, 0.500 mmol) at room temperature under N_2. The reaction mixture was stirred for 3 h. The mixture was quenched with saturated aqueous NH_4Cl (30 mL) and extracted with EtOAc (40 mL × 1), washed with saturated aqueous NH_4Cl (40 mL × 2) and brine (40 mL × 1). The organic layer was dried over Na_2SO_4 and concentrated in vacuo. The crude product was purified by flash column chromatography ($CHCl_3$/MeOH = only $CHCl_3$ to 100/1) to afford **25** (52.4 mg, 0.088 mmol, 88%) as a colorless solid. Mp 221−222 °C. $[\alpha]^{27}_D$ +5.5 (*c* 1.0, MeOH). IR (KBr) ν cm^{-1}: 3386, 3311, 2968, 2937, 2885, 1766, 1736, 1462, 1379, 1317, 1286, 1238, 1169, 1095, 1032, 997, 924, 899, 762. ^{1}H NMR (500 MHz, CD_3OD): 8.40 (s, 1H), 7.68 (s, 1H), 7.11 (s, 1H), 5.92 (s, 1H), 5.38 (dd, *J* = 10.9, 1.2 Hz, 1H), 5.29 (dd, *J* = 11.5, 2.3 Hz, 1H), 4.13 (dd, *J* = 16.0, 2.3 Hz, 1H, H-13), 3.98 (dd, *J* = 16.0, 2.3 Hz), 3.66 (t, *J* = 2.9 Hz, 1H), 3.51 (d, *J* = 2.3 Hz, 1H), 3.44 (d, *J* = 4.0 Hz, 1H), 3.17 (dq, *J* = 13.5, 6.9 Hz, 1H), 2.60 (t, *J* = 2.6 Hz, 1H), 2.44 (m, 1H), 2.18 (m, 1H), 2.03 (m, 1H), 1.93 (m, 1H), 1.72 (dd, *J* = 15.5, 8.6 Hz, 1H), 1.54 (m, 1H), 1.51 (s, 3H), 1.46 (s, 3H), 1.28 (d, *J* = 15.5 Hz, 1H), 1.22 (s, 3H), 1.21 (s, 3H, 6-C$\underline{H}_3$), 1.21 (d, *J* = 6.9 Hz, 3H), 1.18 (d, *J* = 6.9 Hz, 3H), 0.98 (d, *J* = 7.5 Hz, 3H), 0.85 (t, *J* = 7.5 Hz, 3H). ^{13}C NMR (125 MHz, CD_3OD) δ (ppm): 174.5, 150.2, 138.9, 131.0, 119.0, 103.1, 85.1, 85.0, 81.6, 79.7, 78.5, 76.4, 75.3, 74.9, 71.6, 59.1, 44.0, 38.5, 35.6, 33.7, 31.7, 28.0, 26.7, 24.3, 22.5, 20.0, 16.9 (2C), 15.6, 10.9, 8.9. HRMS (ESI$^+$) *m*/*z*: 615.3252 [M + Na]$^+$; calcd for $C_{31}H_{48}N_2NaO_9$, 615.3258. HPLC analysis (method A): retention time = 7.20 min; peak area, 95%.

(9*S*)-9-Dihydro-9,11-*O*-isopropylidene-3-*O*-((4-(*N*-methylcarbamoylguanidyl)butyl)carbamoyl)-5-*O*-propargyl-erythronolide A: 26. To a solution of **25** (30.0 mg, 0.0506 mmol) in THF (0.55 mL) was added dropwise over 15 min a solution of 1,4-diaminobutane (22.3 mg, 0.253 mmol) in THF (0.55 mL). The reaction mixture was stirred at room temperature for 3 h. The mixture was diluted with EtOAc (10 mL) and added to saturated aqueous NH_4Cl (5 mL) and separated. The organic layer was washed with saturated aqueous NH_4Cl (5 mL × 2), and then the organic layer was dried over Na_2SO_4 and concentrated in vacuo. The crude product was used for the next step without further purification. To a solution of the crude product in THF (1.1 mL) were added DIPEA (44.0 μL, 0.253 mmol) and **15** (42.3 mg, 0.253 mmol). The reaction mixture was stirred at 55 °C for 14 h. The crude mixture was concentrated and purified by preparative TLC ($CHCl_3$/MeOH/30% NH_4OH = 7/1/0.1) to afford **26** (22.1 mg, 61% over 2 steps) as a colorless solid. Mp 119−122 °C. $[\alpha]_D^{28}$ +11.4 (*c* 1.0, MeOH). IR (KBr) ν cm^{-1}: 3305, 2968, 2937, 1732, 1724, 1720, 1612, 1514, 1458, 1379, 1255, 1169, 1086, 1032, 754. ^{1}H NMR (500 MHz, CD_3OD) δ (ppm): 5.24 (dd, *J* = 11.5, 2.3 Hz, 1H), 4.98 (dd, *J* = 10.9, 1.2 Hz, 1H), 4.19 (dd, *J* = 16.0, 2.3 Hz, 1H), 4.01 (dd, *J* = 16.0, 2.3 Hz, 1H), 3.63 (t, *J* = 2.9 Hz, 1H), 3.51 (d, *J* = 2.3 Hz, 1H), 3.40−3.21 (m, 4H), 3.27 (d, *J* = 4.0 Hz, 1H), 2.88 (m, 1H), 2.75 (t, *J* = 2.3 Hz, 1H), 2.70 (s, 3H), 2.25 (m, 1H), 2.15 (m, 1H), 2.01 (m, 1H), 1.91 (m, 1H), 1.71 (q, *J* = 15.8, 8.9 Hz, 1H), 1.58−1.45 (m, 1H), 1.49 (s, 3H), 1.43 (s, 3H), 1.35−1.25 (m, 1H), 1.23 (s, 3H), 1.20 (d, *J* = 6.9 Hz, 3H), 1.18 (s, 3H), 1.13 (d, *J* = 6.9 Hz, 3H), 1.04 (d, *J* = 7.5 Hz, 3H), 0.97 (d, *J* = 6.9 Hz, 3H), 0.83 (t, *J* = 7.5 Hz, 3H). ^{13}C NMR (125 MHz, CD_3OD) δ (ppm): 175.4, 159.1, 103.1, 86.5, 81.6, 81.1, 79.9, 78.1, 75.5, 75.2, 75.0, 71.6, 59.2, 44.6, 41.6 (2C), 38.5, 35.6, 33.7, 31.8, 28.0, 26.8, 26.6, 24.2, 22.5, 20.0, 16.91, 16.88, 15.6, 10.8, 9.0 (The peaks of −NH$\underline{C}$(=NH)-NH$\underline{C}$ONHMe were not observed in ^{13}C NMR). HRMS (ESI$^+$) *m*/*z*: 734.4315 [M + Na]$^+$; calcd for $C_{35}H_{61}N_5NaO_{10}$, 734.4316. HPLC analysis (method A): retention time = 6.20 min; peak area, >99%.

(9*S*)-9-Dihydro-9,11-*O*-isopropylidene-3-*O*-((1-(2-(*N*-methylcarbamoylguanidyl)ethyl)-1*H*-1,2,3-triazol-4-yl)-methyl)erythronolide A: 27. According to the preparation of **21**, **23** (50.0 mg, 0.100 mmol) was converted to **27** (47.4 mg, 0.0693 mmol) in 69% yield as a colorless solid. Mp 122−125 °C. $[\alpha]_D^{27}$ +28.6 (*c* 0.41, MeOH). IR (KBr) ν cm^{-1}: 3398, 2972, 2937, 1732, 1620, 1562, 1512, 1462, 1379, 1311, 1227, 1169, 1078, 1032, 920, 756. ^{1}H NMR (500 MHz, CD_3OD) δ (ppm) 7.97 (s. 1H), 5.20 (dd, *J* = 10.9, 2.3 Hz, 1H), 4.91−4.70 (m, 2H), 4.58 (t, *J* = 5.2 Hz, 2H), 3.70 (m, 3H), 3.65 (d, *J* = 2.9 Hz, 1H), 3.52 (t, *J* = 1.7 Hz, 1H), 3.50 (d, *J* = 3.4 Hz, 1H), 2.78 (m, 1H), 2.70 (s, 3H), 2.18 (m, 1H), 2.04−1.96 (m, 2H), 1.89 (m, 1H), 1.76 (m, 1H), 1.55−1.47 (m, 1H), 1.50 (s, 3H), 1.45 (s, 3H), 1.30 (d, *J* = 14.9 Hz, 1H), 1.27 (d, *J* = 6.9 Hz, 3H), 1.23 (s, 3H), 1.21 (d, *J* = 6.9 Hz, 3H), 1.18 (s, 3H), 1.00 (d, *J* = 4.6 Hz, 3H), 0.99 (d, *J* = 5.2 Hz, 3H), 0.83 (t, *J* = 7.5 Hz, 3H). ^{13}C NMR (125 MHz, CD_3OD) δ (ppm) 176.5, 146.3, 125.6, 103.0, 88.0, 81.7, 80.8, 77.9, 76.0, 75.0, 71.7, 67.2, 50.8, 46.0, 41.7, 39.5, 35.1, 33.9, 31.9, 28.0, 26.8, 26.6, 24.3, 22.5, 19.9, 16.9 (2C), 16.3, 10.8, 9.4 (The peaks of −NH$\underline{C}$(=NH)NH$\underline{C}$ONHMe were not observed in ^{13}C NMR). HRMS (ESI$^+$)

DOI: 10.1021/acs.jmedchem.5b00175
J. Med. Chem. XXXX, XXX, XXX−XXX

m/z: 706.4115 [M + Na]$^+$; calcd for $C_{32}H_{57}N_7NaO_9$, 706.4115. HPLC analysis (method A): retention time = 5.17 min; peak area, >99%.

(9*S*)-9-Dihydro-9,11-*O*-isopropylidene-3-*O*-((2-(*N*-methylcarbamoylguanidino)ethyl)carbamoyl)-5-*O*-propargylerythronolide A: 29. According to the preparation of **26**, **25** (30.0 mg, 0.0506 mmol) and ethylenediamine (16.9 μL, 0.253 mmol) were converted to the product **29** (13.7 mg, 39% over 2 steps) as a colorless solid. Mp 124−127 °C. $[\alpha]_D^{24}$ +11.6 (*c* 0.98, MeOH). IR (KBr) ν cm^{-1}: 3309, 2966, 2929, 1734, 1614, 1510, 1462, 1381, 1260, 1170, 1109, 1088, 1034, 760. ^{1}H NMR (500 MHz, CD_3OD) δ (ppm): 5.25 (dd, *J* = 11.2, 2.0 Hz, 1H), 4.98 (dd, *J* = 10.9, 1.6 Hz, 1H), 4.19 (dd, *J* = 15.5, 2.3 Hz, 1H), 4.01 (dd, *J* = 15.5, 2.3 Hz, 1H), 3.63 (app s, 1H), 3.50 (d, *J* = 1.7 Hz, 1H), 3.36−3.23 (complex m, 5H), 2.88 (m, 1H), 2.76 (t, *J* = 2.3 Hz, 1H), 2.69 (s, 3H), 2.25 (m, 1H), 2.16 (m, 1H), 2.01 (m, 1H), 1.91 (m, 1H), 1.72 (dd, *J* = 15.2, 8.9 Hz, 1H), 1.51 (m, 1H), 1.49 (s, 3H), 1.43 (s, 3H), 1.28 (m, 1H), 1.23 (s, 3H), 1.20 (d, *J* = 7.5 Hz, 3H), 1.18 (s, 3H), 1.13 (d, *J* = 6.9 Hz, 3H), 1.04 (d, *J* = 7.5 Hz, 3H), 0.97 (d, *J* = 7.4 Hz, 3H), 0.83 (t, *J* = 7.5 Hz, 3H). ^{13}C NMR (125 MHz, CD_3OD) δ (ppm): 175.4, 161.0, 159.1, 103.1, 86.5, 81.6, 81.1, 79.9, 78.1, 75.5, 75.2, 75.0, 71.6, 59.2, 44.6, 41.6 (2C), 38.5, 35.6, 33.7, 31.8, 28.0, 26.8, 26.6, 24.2, 22.5, 20.0, 16.91, 16.88, 15.6, 10.8, 9.0 (The peak of −NHC(═NH)NHCONHMe was not observed in ^{13}C NMR). HRMS (ESI$^+$) *m/z*: 706.4011 [M + Na]$^+$; calcd for $C_{33}H_{57}N_5NaO_{10}$, 706.4003. HPLC analysis (method A): retention time = 6.00 min; peak area, 95%.

(9*S*)-9-Dihydro-9,11-*O*-isopropylidene-3-*O*-((3-(*N*-methylcarbamoylguanidino)propyl)carbamoyl)-5-*O*-propargylerythronolide A: 30. According to the preparation of **26**, **25** (160.7 mg, 0.271 mmol) and 1,3-diaminopropane (220 μL, 2.71 mmol) were converted to the product **30** (62.5 mg, 0.090 mmol, 33% over 2 steps) as a colorless solid. Mp 119−122 °C. $[\alpha]_D^{26}$ +11.8 (*c* 1.0, MeOH). IR (KBr) ν cm^{-1}: 3359, 3305, 2970, 1732, 1616, 1514, 1458, 1379, 1259, 1169, 1086, 1032, 756. ^{1}H NMR (500 MHz, CD_3OD) δ (ppm): 5.25 (dd, *J* = 11.5, 2.3 Hz, 1H), 4.98 (dd, *J* = 11.0, 1.8 Hz, 1H), 4.20 (dd, *J* = 15.5, 2.3 Hz, 1H), 4.01 (dd, *J* = 15.5, 2.3 Hz, 1H), 3.63 (dd, *J* = 2.9, 2.9 Hz, 1H), 3.51 (d, *J* = 2.3 Hz, 1H), 3.27 (d, *J* = 3.4 Hz, 1H), 3.23 (m, 2H), 3.19 (t, *J* = 6.9 Hz, 2H), 2.89 (m, 1H), 2.76 (t, *J* = 2.3 Hz, 1H), 2.69 (s, 3H), 2.25 (m, 1H), 2.16 (m, 1H), 2.01 (m, 1H), 1.91 (m, 1H), 1.77−1.69 (complex m, 3H), 1.51 (m, 1H), 1.49 (s, 3H), 1.43 (s, 3H), 1.26 (m, 1H), 1.23 (s, 3H), 1.20 (d, *J* = 6.9 Hz, 3H), 1.19 (s, 3H), 1.13 (d, *J* = 6.3 Hz, 3H), 1.05 (d, *J* = 7.5 Hz, 3H), 0.97 (d, *J* = 7.5 Hz, 3H), 0.83 (t, *J* = 7.5 Hz, 3H). ^{13}C NMR (125 MHz, CD_3OD) δ (ppm): 175.4, 167.1 (detected by HMBC), 160.6, 158.9, 103.1, 86.6, 81.6, 81.1, 79.7, 78.1, 75.5, 75.2, 75.0, 71.5, 59.2, 44.6, 39.1 (2C), 38.5, 35.6, 33.7, 31.8, 30.8, 27.9, 26.8, 26.6, 24.2, 22.5, 20.0, 16.90, 16.88, 15.6, 10.9, 9.0. HRMS (ESI$^+$) *m/z*: 698.4327 [M + H]$^+$; calcd for $C_{34}H_{60}N_5O_{10}$, 698.4340. HPLC analysis (method B): retention time = 25.8 min; peak area, 97%.

(9*S*)-9-Dihydro-9,11-*O*-isopropylidene-3-*O*-((5-(*N*-methylcarbamoylguanidino)pentyl)carbamoyl)-5-*O*-propargylerythronolide A: 31. According to the preparation of **26**, **25** (35.1 mg, 0.0592 mmol) and 1,5-diaminopentane (27.8 μL, 0.237 mmol) were converted to the product **31** (14.5 mg, 0.0199 mmol, 34% over 2 steps) as a colorless solid. Mp 107−110 °C. $[\alpha]_D^{22}$ +10.6 (*c* 0.73, MeOH). IR (KBr) ν cm^{-1}: 3388, 3305, 2968, 2933, 1736, 1608, 1512, 1458, 1379, 1261, 1169, 1088, 1032, 800. ^{1}H NMR (500 MHz, CD_3OD) δ (ppm): 5.24 (dd, *J* = 11.2, 2.6 Hz, 1H), 4.97 (d, *J* = 11.5 Hz, 1H), 4.20 (dd, *J* = 15.5, 2.3 Hz, 1H), 4.00 (dd, *J* = 15.5, 2.3 Hz, 1H), 3.63 (t, *J* = 2.9 Hz, 1H), 3.51 (d, *J* = 1.7 Hz, 1H), 3.26 (d, J = 3.4 Hz, 1H), 3.20−3.09 (m, 3H), 2.89 (m, 1H), 2.76 (t, *J* = 2.3 Hz, 1H), 2.69 (s, 3H), 2.25 (m, 1H), 2.16 (m, 1H), 2.00 (m, 1H), 1.91 (m, 1H), 1.71 (m, 1H), 1.62−1.46 (m, 3H), 1.49 (s, 3H), 1.46−1.25 (m, 5H), 1.43 (s, 3H), 1.23 (s, 3H), 1.20 (d, *J* = 6.9 Hz, 3H), 1.18 (s, 3H), 1.12 (d, *J* = 6.9 Hz, 3H), 1.04 (d, *J* = 8.0 Hz, 3H), 0.99−0.86 (m, 1H), 0.97 (d, *J* = 7.5 Hz, 3H), 0.83 (t, *J* = 7.5 Hz, 3H). ^{13}C NMR (125 MHz, CD_3OD) δ (ppm): 175.4, 160.8, 158.8, 103.1, 86.9, 81.6, 81.1, 79.6, 78.1, 75.4, 75.2, 75.0, 71.6, 59.3, 44.7, 41.8, 41.7, 38.5, 35.6, 33.7, 31.8, 30.5, 29.8, 27.9, 26.8, 26.6, 25.0, 24.2, 22.5, 20.0, 16.91, 16.88, 15.6, 10.9, 9.1 (The peak of −NHC(═NH)NHCONHMe was not observed in ^{13}C NMR). HRMS (ESI$^+$) *m/z*: 726.4642 [M + H]$^+$; calcd for $C_{36}H_{64}N_5O_{10}$: 726.4653. HPLC analysis (method A): retention time = 6.12 min; peak area, >99%.

(9*S*)-9-Dihydro-9,11-*O*-isopropylidene-3-*O*-((7-(*N*-methylcarbamoylguanidino)heptyl)carbamoyl)-5-*O*-propargylerythronolide A: 32. According to the preparation of **26**, **25** (33.8 mg, 0.0570 mmol) and 1,7-diaminoheptane (138.4 mg, 1.06 mmol) were converted to the product **32** (9.6 mg, 0.0127 mmol, 22% over 2 steps) as a colorless solid. Mp 100−105 °C. $[\alpha]_D^{27}$ +13.7 (*c* 0.57, MeOH). IR (KBr) ν cm^{-1}: 3309, 2960, 2927, 2856, 1732, 1539, 1462, 1379, 1259, 1169, 1088, 1032, 802, 758. ^{1}H NMR (500 MHz, CD_3OD) δ (ppm): 5.24 (dd, *J* = 11.5, 2.3 Hz, 1H), 4.96 (d, *J* = 10.9 Hz, 1H), 4.20 (dd, *J* = 15.8, 2.0 Hz, 1H), 3.99 (dd, *J* = 15.5, 2.3 Hz, 1H), 3.63 (t, *J* = 2.6 Hz, 1H), 3.51 (d, *J* = 2.3 Hz, 1H), 3.24 (d, *J* = 3.4 Hz, 1H), 3.21 (t, *J* = 7.2 Hz, 2H), 3.15−3.10 (m, 2H), 2.89 (m, 1H), 2.76 (t, *J* = 2.3 Hz, 1H), 2.73 (s, 3H), 2.24 (m, 1H), 2.17 (m, 1H), 2.10−1.97 (m, 2H), 1.95−1.85 (m, 2H), 1.72 (m, 1H), 1.66−1.56 (m, 3H), 1.56−1.45 (m, 3H), 1.49 (s, 3H), 1.43 (s, 3H), 1.41−1.25 (m, 10H), 1.23 (s, 3H), 1.20 (d, *J* = 6.9 Hz, 3H), 1.19 (s, 3H), 1.12 (d, *J* = 6.9 Hz, 3H), 1.05 (d, *J* = 7.5 Hz, 3H), 0.97 (d, *J* = 7.5 Hz, 3H), 0.83 (t, *J* = 7.2 Hz, 3H). ^{13}C NMR (125 MHz, CD_3OD) δ (ppm): 175.4, 158.9, 103.1, 87.0, 81.6, 81.1, 79.5, 78.1, 75.4, 75.2, 75.0, 71.6, 59.4, 44.7, 42.0, 41.8, 38.5, 35.6, 33.7, 31.8, 30.8, 30.0 (2C), 27.9, 27.79, 27.76, 26.8, 26.6, 24.2, 22.5, 20.0, 16.91, 16.88, 15.6, 10.9, 9.1 (The peaks of -NHC(═NH)NHCONHMe were not observed in ^{13}C NMR). HRMS (ESI$^+$) *m/z*: 754.4974 [M + H]$^+$; calcd for $C_{38}H_{68}N_5O_{10}$, 754.4966. HPLC analysis (method A): retention time = 6.45 min; peak area, 97%.

(9*S*)-9-Dihydro-3-*O*-((3-(*N*-methylcarbamoylguanidino)-propyl)carbamoyl)-5-*O*-propargylerythronolide A: 33. To a solution of compound **30** (18.1 mg, 0.0287 mmol) was added 90% aq AcOH (0.57 mL). The reaction mixture was stirred at 100 °C for 11.5 h. The mixture was lowered to room temperature and concentrated in vacuo. The crude materials were purified by TLC chromatography ($CHCl_3$/MeOH/30% NH_4OH = 7/1/0.1) to afford **33** (8.2 mg, 0.012 mmol, 44%) as a colorless solid. Mp 97−101 °C. $[\alpha]_D^{23}$ +7.9 (*c* 0.55, MeOH). IR (KBr) ν cm^{-1}: 3309, 2962, 2933, 1722, 1610, 1527, 1462, 1410, 1379, 1350, 1261, 1171, 1086, 1034, 758. ^{1}H NMR (500 MHz, CD_3OD) δ (ppm): 5.34 (dd, *J* = 10.9, 2.3 Hz, 1H), 4.90 (m, 1H), 4.20 (dd, *J* = 16.0, 2.3 Hz, 1H), 4.04 (dd, *J* = 15.5, 2.3 Hz, 1H), 3.72 (s, 1H), 3.35 (d, *J* = 2.3 Hz, 1H), 3.28−3.19 (m, 2H), 3.26 (d, *J* = 4.0 Hz, 1H), 3.21 (dt, *J* = 6.7, 1.6 Hz, 1H), 2.89 (m, 1H), 2.78 (t, *J* = 2.3 Hz, 1H), 2.71 (s, 3H), 2.28 (m, 1H), 2.11 (m, 1H), 1.97 (m, 1H), 1.93 (m, 1H), 1.84−1.70 (complex m, 2H), 1.54 (dd, *J* = 15.2, 8.3 Hz, 1H), 1.50 (m, 1H), 1.36−1.26 (m, 1H), 1.30 (s, 3H), 1.21 (dd, *J* = 15.5, 2.3 Hz, 3H), 1.16 (d, *J* = 6.9 Hz, 3H), 1.14 (s, 3H), 1.11 (d, *J* = 6.3 Hz, 3H), 1.04 (d, *J* = 7.5 Hz, 3H), 0.98 (d, *J* = 6.9 Hz, 3H), 0.84 (t, *J* = 7.5 Hz, 3H). ^{13}C NMR (125 MHz, CD_3OD) δ (ppm): 175.7, 159.1, 86.8, 83.6, 81.1, 79.8, 78.5, 76.4, 75.6, 75.5, 72.4, 59.4, 44.6, 39.3, 39.1, 37.9, 36.0 (2C), 33.3, 30.6, 26.8, 26.2, 22.8, 21.2, 17.7, 17.0, 15.2, 11.1, 8.8 (The peaks of −NHC(═NH)-NHCONHMe were not observed in ^{13}C NMR). HRMS (ESI$^+$) *m/z*: 680.3834 [M + Na]$^+$; calcd for $C_{31}H_{55}N_5NaO_{10}$, 680.3847. HPLC analysis (method A): retention time = 5.42 min; peak area, 99%.

Procedures for the Expression and Preparation of Each *Sm*ChiB.[37] A *Sm*ChiB gene was inserted into a pUC119 vector for expression. *Escherichia coli* DH5a harboring plasmid pMCB7 (carrying the *Sm*ChiB gene) were grown at 37 °C in LB medium containing 50 μg/mL ampicillin and 0.5 mM isopropylthio-β-D-galactoside (IPTG) for 24 h and collected by centrifugation. The harvested cells were suspended in 100 mM phosphate buffer (pH 7.0) and disrupted by sonication on ice. After centrifugation, the supernatant was used as crude *Sm*ChiB. Chitinolytic activity was assayed in 100 mM phosphate buffer (pH 7.0) at 37 °C using a fluorescent oligosaccharide, 4-methylumbelliferyl β-D-*N*,*N*′-diacetylchitobiosidehydrate [4MU-$(GlcNAc)_2$, Sigma]. According to standard procedures, expression of *Sm*ChiB was evaluated and chitinolytic activity assayed.

Chitinolytic activity of *S. marcescens* Chitinase.[37] Chitinolytic activity of *Sm*ChiB was assayed by the use of 50 μL of 80 μM 4MU-$(GlcNAc)_2$ and 30 μL of *Sm*ChiB solution in 100 mM phosphate buffer, pH 7.0 (total volume 100 μL in one wall), at 37 °C.

DOI: 10.1021/acs.jmedchem.5b00175
J. Med. Chem. XXXX, XXX, XXX−XXX

Fluorescence (excitation at 355 nm, emission at 460 nm) was measured at intervals of 60 s. It was also confirmed that crude *Sm*ChiB did not convert 4-methylumbelliferyl β-D-*N*,*N*′,*N*′-triacetylchitotrioside hydrate [4MU-$(GlcNAc)_3$, Sigma] to 4-methylumbelliferone (4MU).

Procedures for IC_{50} Measurements against *Sm*ChiB.[37] Amounts of 10 μL of 0.1 M phosphate buffer (pH 7.0), 10 μL of each inhibitors in MeOH, 30 μL of diluted crude chitinase solution (*Sm*ChiB, ×40 dilution with 0.1 M phosphate buffer, pH 7.0) (see the procedures for the preparation of *Sm*ChiB), and 50 μL of 80 μM 4-methylumberiferyl-β-D-*N*,*N*′-diacetylchitobiose [4-MU-$(GluNAc)_2$, Sigma] in 0.1 M phosphate buffer (pH 7.0) were placed in each well of a microplate and incubated with 10 μL of inhibitors in MeOH for 5 min. Fluorescence (excitation at 355 nm, emission at 460 nm) was measured at intervals of 60 s by fluorometer (Fluoroscan II, Labsystems (MIC Group, Inc. (GMI), MN, USA)), and the rate of 4-methylumbelliferone production was corrected by calibrating the quenching ratio of each inhibitor using the mixture of the inhibitors and 4MU.

IC_{50} values of all inhibitors against each *Sm*ChiB were determined from dose−response sigmoidal curves, which were calculated using KaleidaGraph (Synergy Software Inc., PA, USA) and the experimental data (Figure S7).[53]

Structural Studies of *Sm*ChiB Complexed with Macrolides 26, 29, 30, 31, 32, and 33.[37,50,53] The crystals of apo-*Sm*ChiB were grown as previously described.[50] Briefly, the protein solution (8 mg mL^{-1}) was mixed with reservoir solution [0.1 M sodium phosphate, pH 7.0, 0.8 M ammonium sulfate, 5% (v/v) glycerol] by 1:1 and set up for the hanging-drop method at 298 K. All inhibitors were prepared as 4 mM solution in 100% methanol and then incorporated into the apo-crystals by soaking. The crystals were flash-cooled by liquid nitrogen and diffraction data collected at the Photon Factory BL-17A (Tsukuba, Japan). The data were processed with iMosflm followed by Scala in ccp4i package.[67] The structures were identified by molecular replacement calculated by Molrep[67] using apo-*Sm*ChiB structure (PDB code 3WD0) as the search model. The refinement of *Sm*ChiB structures was done with Refmac5,[67] and the models were manually fixed with Coot.[68] All the energy restriction files for the macrolide inhibitors were prepared with the JLigand program.[69]

■ ASSOCIATED CONTENT

Supporting Information

Spectra data of all synthesized compounds; structural alignment calculation of NMR structures of **1** and chitinase-bound conformation of **10**; molecular dynamics (MD) simulations and MM-PBSA calculations of **26**, **29**, **30**, **31**; data collection and refinement statistics for the crystals of the *Sm*ChiB complexed with **26** and **29**−**33**; figures of sigmoid curve of **14**, **21**, **24**, **26**, **27**, and **29**−**33**. The Supporting Information is available free of charge on the ACS Publications website at DOI: 10.1021/acs.jmedchem.5b00175.

■ AUTHOR INFORMATION

Corresponding Authors

*S.Ō.: e-mail, omuras@insti.kitasato-u.ac.jp; phone and fax, (+81) 3-5791-6340.

*T.S.: e-mail, sunazuka@lisci.kitasato-u.ac.jp; phone and fax; (+81) 3-5791-6340.

Present Address

#H.G.: School of Pharmacy, Showa University, 1-5-8 Hatanodai, Shinagawa-ku, Tokyo, 142-8555, Japan.

Author Contributions

⊥A.S., N.M., and H.G. contributed equally to this work.

Notes

The authors declare no competing financial interest.

■ ACKNOWLEDGMENTS

We are thankful for Grant for the 21st Century COE Program, a Grant-in-Aid for Scientific Research on Innovative Areas "Chemical Biology of Natural Products" (Grants 24102527, 26102737 to A.S.), KAKENHI (Grant 24590058, to H.G.), together with funds from the Quality Assurance Framework of Higher Education from The Ministry of Education, Culture, Sports, Science and Technology (MEXT), Japan, plus a Cooperative Research Grant of the Institute for Enzyme Research, Joint Usage/Research Center, The University of Tokushima (to T.S.), and a Kitasato University Research Grant for Young Researchers (to A.S.) for supporting this work. We also thank Dr. Hidehito Matsui and Prof. Hideaki Hanaki (Kitasato University) for measurement of antibacterial activity, as well as Dr. Kenichiro Nagai, Noriko Sato, Dr. Takuji Nakashima, Kei Fujisawa, and Sou Ukiyama (Kitasato University) for various instrumental analyses.

■ DEDICATION

The paper is dedicated to Professor Amos B. Smith, III, on the occasion of his 70th birthday.

■ ABBREVIATIONS USED

AcOH, acetic acid; AMCase, acidic mammalian chitinase; Boc, *tert*-butoxycarbonyl; CDI, 1,1′-carbonyldiimidazole; $Cu(PF_6)$-(MeCN), tetrakis(acetonitrile)copper(I) hexafluorophosphate; DCM, dichloromethane; DIPEA, *N*,*N*-diisopropylethylamine; DMF, *N*,*N*-dimethylformamide; EMA, erythromycin A; GlcNAc, *N*-acetylglucosamine; GMS, gastrointestinal motor-stimulating; HCHT, human chitotrioside; HPLC, high performance liquid chromatography; K_2CO_3, potassium carbonate; NaH, sodium hydride; NaN_3, sodium azide; MD, molecular dynamics; MeCN, acetonitrile; MIC, minimum inhibitory concentration; MM-PBSA, molecular mechanics Poisson−Boltzmann surface area; MSSA, methicillin-sensitive *Staphylococcus aureus*; MRSA, methicillin-resistant *Staphylococcus aureus*; 4MU, 4-methylumbelliferone; *Sm*ChiB, *Serratia marcescens* chitinase B; TBAI, tetrabutylammonium iodide; TBTA, tris[(1-benzyl-1*H*-1,2,3-triazol-4-yl)methyl]amine; TFA, trifluoroacetic acid; THF, tetrahydrofuran; VISA, vancomycin-intermediate *Staphylococcus aureus*; VRE, vancomycin-resistant *Enterococci*.

■ REFERENCES

(1) Mcguire, J. M.; Bunch, R. L.; Anderson, R. C.; Boaz, H. E.; Flynn, E. H.; Powell, H. M.; Smith, J. W. "Ilotycin," a new antibiotic. *Antibiot. Chemother.* **1952**, *2*, 281−283.

(2) Ōmura, S., Ed. *Macrolide Antibiotics. Chemistry, Biology, and Practice*, 2nd ed.; Academic Press: Amsterdam, 2002.

(3) Itoh, Z.; Nakaya, M.; Suzuki, H.; Arai, H.; Wakabayashi, K. Erythromycin mimics exogenous motilin in gastrointestinal contractile activity in the dog. *Am. J. Physiol.* **1984**, *247*, G688−G694.

(4) Kudoh, S.; Uetake, T.; Hagiwara, K.; Hirayama, M.; Hus, L. H.; Kimura, H.; Sugiyama, Y. Clinical effects of low-dose long-term erythromycin chemotherapy on diffuse panbronchiolitis. *Jpn. J. Thorac. Dis.* **1987**, *25*, 632−642 (in Japanese with English abstract).

(5) Shinkai, M.; Henke, M. O.; Rubin, B. K. Macrolide antibiotics as immunomodulatory medications: proposed mechanisms of action. *Pharmacol. Ther.* **2008**, *117*, 393−405.

(6) Tarran, R.; Sabater, J. R.; Clarke, T. C.; Tan, C. D.; Davies, C. M.; Liu, J.; Yeung, A.; Garland, A. L.; Stutts, M. J.; Abraham, W. M.; Phillips, G.; Baker, W. R.; Wright, C. D.; Wilbert, S. Nonantibiotic macrolides prevent human neutrophil elastase-induced mucus stasis

DOI: 10.1021/acs.jmedchem.5b00175
J. Med. Chem. XXXX, XXX, XXX−XXX

and airway surface liquid volume depletion. *Am. J. Physiol.: Lung Cell. Mol. Physiol.* **2013**, *304*, L746−L756.

(7) Mencarelli, A.; Distrutti, E.; Renga, B.; Cipriani, S.; Palladino, G.; Booth, C.; Tudor, G.; Guse, J.-H.; Hahn, U.; Burnet, M.; Fiorucci, S. Development of non-antibiotic macrolide that corrects inflammation-driven immune dysfunction in models of inflammatory bowel diseases and arthritis. *Eur. J. Pharmacol.* **2011**, *665*, 29−39.

(8) Ōmura, S.; Tsuzuki, K.; Sunazuka, T.; Toyoda, H.; Takahashi, I.; Itoh, Z. Gastrointestinal motor-stimulating activity of macrolide antibiotics and the structure-activity relationship. *J. Antibiot.* **1985**, *38*, 1631−1632.

(9) Ōmura, S.; Tsuzuki, K.; Sunazuka, T.; Marui, S.; Toyoda, H.; Inatomi, N.; Itoh, Z. Macrolides with gastrointestinal motor stimulating activity. *J. Med. Chem.* **1987**, *30*, 1941−1943.

(10) Tsuzuki, K.; Sunazuka, T.; Marui, S.; Toyoda, H.; Ōmura, S. Motilides, macrolides with gastrointestinal motor stimulating activity. I. O-Substituted and tertiary N-substituted derivatives of 8,9-anhydroerythromycin A 6,9-hemiacetal. *Chem. Pharm. Bull.* **1989**, *37*, 2687−2700.

(11) Sunazuka, T.; Tsuzuki, K.; Marui, S.; Toyoda, H.; Ōmura, S.; Inatomi, N.; Itoh, Z. Motilides, macrolides with gastrointestinal motor stimulating activity. II. Quaternary N-substituted derivatives of 8,9-anhydroerythromycin A 6,9-hemiacetal and 9,9-dihydroerythromycin A 6,9-epoxide. *Chem. Pharm. Bull.* **1989**, *37*, 2701−2709.

(12) Sugawara, A.; Sueki, A.; Hirose, T.; Nagai, K.; Gouda, H.; Hirono, S.; Shima, H.; Akagawa, K. S.; Ōmura, S.; Sunazuka, T. Novel 12-membered non-antibiotic macrolides from erythromycin A; EM900 series as novel leads for anti-inflammatory and/or immunomodulatory agents. *Bioorg. Med. Chem. Lett.* **2011**, *21*, 3373−3376.

(13) Hashimoto, Y. Thalidomide as a multi-template for development of biologically active compounds. *Arch. Pharm. Chem. Life Sci.* **2008**, *341*, 536−547.

(14) Deshpande, M. V.; O'Donnell, R.; Gooday, G. W. Regulation of chitin synthase activity in the dimorphic fungus *Benjaminiella poitrasii* by external osmotic pressure. *FEMS Microbiol. Lett.* **1997**, *152*, 327−332.

(15) Kuranda, M. J.; Robbins, P. W. Chitinase is required for cell separation during growth of *Saccharomyces cerevisiae*. *J. Biol. Chem.* **1991**, *266*, 19758−19767.

(16) Merzendorfer, H.; Zimoch, L. Chitin metabolism in insects: structure, function and regulation of chitin synthases and chitinases. *J. Exp. Biol.* **2003**, *206*, 4393−4412.

(17) Henrissat, B.; Bairoch, A. New families in the classification of glycosyl hydrolases based on amino acid sequence similarities. *Biochem. J.* **1993**, *293*, 781−788.

(18) Terwisscha van Scheltinga, A. C.; Hennig, M.; Dijikstra, B. W. The 1.8 Å resolution structure of hevamine, a plant chitinase/lysozyme, and analysis of the conserved sequence and structure motifs of glycosyl hydrolase family 18. *J. Mol. Biol.* **1996**, *262*, 243−257.

(19) Andersen, O. A.; Dixon, M. J.; Eggleston, I. M.; van Aalten, D. M. F. Natural product family 18 chitinase inhibitors. *Nat. Prod. Rep.* **2005**, *22*, 563−579.

(20) Sutherland, T. E.; Maizels, R. M.; Allen, J. E. Chitinases and chitinase-like proteins: potential therapeutic targets for the treatment of T-helper type 2 allergies. *Clin. Exp. Allergy* **2009**, *39*, 943−955.

(21) Zhu, Z.; Zheng, T.; Homer, R. J.; Kim, Y.-K.; Chen, N. Y.; Cohn, L.; Hamid, Q.; Elias, J. A. Acidic mammalian chitinase in asthmatic Th2 inflammation and IL-13 pathway activation. *Science* **2004**, *304*, 1678−1682.

(22) Musumeci, S., Paoletti, M. G., Eds. *Binomium Chitin-Chitinase Recent Issues*; Nova Biochemical Books: Hauppauge NY, 2009 and references therein.

(23) Gloeckner, C.; Garner, A. L.; Mersha, F.; Oksov, Y.; Tricoche, N.; Eubanks, L. M.; Lustigman, S.; Kaufmann, G. F.; Janda, K. D. Repositioning of an existing drug for the neglected tropical disease onchocerciasis. *Proc. Natl. Acad. Sci. U.S.A.* **2010**, *107*, 3424−3429.

(24) Gooyit, M.; Tricoche, N.; Lustigman, S.; Janda, K. D. Dual protonophore-chitinase inhibitors dramatically affect *O. volvulus* molting. *J. Med. Chem.* **2014**, *57*, 5792−5799.

(25) Sakuda, S.; Isogai, A.; Matsumoto, S.; Suzuki, A.; Koseki, K. Structure of allosamisin, a novel insect chitinase inhibitor, produced by *Streptomyces* sp. *Tetrahedron Lett.* **1986**, *27*, 2475−2478.

(26) Sakuda, S. Studies on the chitinase inhibitors, allosamidins. In *Chitin Enzymology*; Muzzarelli, R. A. A., Ed.; Atec Edizioni: Grottammare, Italy, 1996; Vol. 2, pp 203−212.

(27) Kato, T.; Shizuri, Y.; Izumida, H.; Yokoyama, A.; Endo, M. Styloguanidines, new chitinase inhibitors from the marine sponge *Stylotella aurantium*. *Tetrahedron Lett.* **1995**, *36*, 2133−2136.

(28) Izumida, H.; Imamura, N.; Sano, H. A novel chitinase inhibitor from a marine bacterium, *Pseudomonas* sp. *J. Antibiot.* **1996**, *76*, 76−80.

(29) Takadera, T.; Nomoto, A.; Izumida, H.; Nishijima, M.; Sano, H. The effect of chitinase inhibitors, cyclo(Arg-Pro) against cell separation of *Saccharomyces cerevisiae* and the morphological change of *Candida albicans*. *J. Antibiot.* **1996**, *49*, 829−831.

(30) Houston, D. R.; Eggleston, I.; Synstad, B.; Eijsink, V. G. H.; van Aalten, D. M. F. The cyclic dipeptide CI-4 [cyclo-(L-Arg-D-Pro)] inhibits family 18 chitinases by structural mimicry of a reaction intermediate. *Biochem. J.* **2002**, *368*, 23−27.

(31) Quinoa, E.; Crews, P. Phenolic constituent of *Psammaplysilla*. *Tetrahedron Lett.* **1987**, *28*, 3229−3232.

(32) Arabshahi, L.; Schmitz, F. J. Brominated tyrosine metabolites from an unidentified sponge. *J. Org. Chem.* **1987**, *52*, 3584−3586.

(33) Ōmura, S.; Arai, N.; Yamaguchi, Y.; Masuma, R.; Iwai, Y.; Namikoshi, M.; Turberg, A.; Kölbl, H.; Shiomi, K. Argifin, a new chitinase inhibitor, produced by *Gliocladium* sp. FTD-0668. I. Taxonomy, fermentation, and biological activities. *J. Antibiot.* **2000**, *53*, 603−608.

(34) Arai, N.; Shiomi, K.; Iwai, Y.; Ōmura, S. Argifin, a new chitinase inhibitor, produced by *Gliocladium* sp. FTD-0668. II. Isolation, physico-chemical properties, and structure elucidation. *J. Antibiot.* **2000**, *53*, 609−614.

(35) Shiomi, K.; Arai, N.; Iwai, Y.; Turberg, A.; Kölbl, H.; Ōmura, S. Structure of argifin, a new chitinase inhibitor produced by *Gliocladium* sp. *Tetrahedron Lett.* **2000**, *41*, 2141−2143.

(36) Arai, N.; Shiomi, K.; Yamaguchi, Y.; Masuma, R.; Iwai, Y.; Turberg, A.; Kölbl, H.; Ōmura, S. Argadin, a new chitinase inhibitor, produced by *Clonostachys* sp. FO-7314. *Chem. Pharm. Bull.* **2000**, *48*, 1442−1446.

(37) Hirose, T.; Sunazuka, T.; Sugawara, A.; Endo, A.; Iguchi, K.; Yamamoto, T.; Ui, H.; Shiomi, K.; Watanabe, T.; Sharpless, K. B.; Ōmura, S. Chitinase inhibitors: extraction of the active framework from natural argifin and use of in situ click chemistry. *J. Antibiot.* **2009**, *62*, 277−282.

(38) Houston, D. R.; Shiomi, K.; Arai, N.; Ōmura, S.; Peter, M. G.; Turberg, A.; Synstad, B.; Eijsink, V. G. H.; van Aalten, D. M. F. High-resolution structures of a chitinase complexed with natural product cyclopentapeptide inhibitors: mimicry of carbohydrate substrate. *Proc. Natl. Acad. Sci. U.S.A.* **2002**, *99*, 9127−9132.

(39) Rao, F. V.; Houston, D. R.; Boot, R. G.; Aerts, J. M.; Hodkinson, M.; Adams, D. J.; Shiomi, K.; Ōmura, S.; van Aalten, D. M. F. Specificity and affinity of natural product cyclopentapeptide inhibitors against *A. fumigatus*, human, and bacterial chitinases. *Chem. Biol.* **2005**, *12*, 65−76.

(40) Anderson, O. A.; Nathubhai, A.; Dixon, M. J.; Eggleston, I. M.; van Aalten, D. M. F. Structure-based dissection of the natural product cyclopentapeptide chitinase inhibitor argifin. *Chem. Biol.* **2008**, *15*, 295−301.

(41) Dixon, M. J.; Anderson, O. A.; van Aalten, D. M. F.; Eggleston, I. M. An efficient synthesis of argifin: a natural product chitinase inhibitor with chemotherapeutic potential. *Bioorg. Med. Chem. Lett.* **2005**, *15*, 4717−4721.

(42) Dixon, M. J.; Nathubhai, A.; Anderson, O. A.; van Aalten, D. M. F.; Eggleston, I. M. Solid-phase synthesis of cyclic peptide chitinase inhibitors: SAR of the argifin scaffold. *Org. Biomol. Chem.* **2009**, *7*, 259−268.

(43) Gouda, H.; Yanai, Y.; Sugawara, A.; Sunazuka, T.; Ōmura, S.; Hirono, S. Computational analysis of the binding affinities of the

DOI: 10.1021/acs.jmedchem.5b00175
J. Med. Chem. XXXX, XXX, XXX−XXX

natural-product cyclopentapeptides argifin and argadin to chitinase B from *Serratia marcescens*. *Bioorg. Med. Chem.* **2008**, *16*, 3565−3579.

(44) Gouda, H.; Sunazuka, T.; Iguchi, K.; Sugawara, A.; Hirose, T.; Noguchi, Y.; Saito, Y.; Yanai, Y.; Yamamoto, T.; Watanabe, T.; Shiomi, K.; Ōmura, S.; Hirono, S. Computer-aided rational molecular design of argifin-derivatives with increased inhibitory activity against chitinase B from *Serratia marcescens*. *Bioorg. Med. Chem. Lett.* **2009**, *19*, 2630−2633.

(45) Gouda, H.; Terashima, S.; Iguchi, K.; Sugawara, A.; Saito, Y.; Yamamoto, T.; Hirose, T.; Shiomi, K.; Sunazuka, T.; Ōmura, S.; Hirono, S. Molecular modeling of human acidic mammalian chitinase in complex with the natural-product cyclopentapeptide chitinase inhibitor argifin. *Bioorg. Med. Chem.* **2009**, *17*, 6270−6278.

(46) Sunazuka, T.; Sugawara, A.; Iguchi, K.; Hirose, T.; Nagai, K.; Noguchi, Y.; Saito, Y.; Yamamoto, T.; Ui, H.; Gouda, H.; Shiomi, K.; Watanabe, T.; Ōmura, S. Argifin; efficient solid phase total synthesis and evaluation of analogues of acyclic peptide. *Bioorg. Med. Chem.* **2009**, *17*, 2751−2758.

(47) Gouda, H.; Sunazuka, T.; Hirose, T.; Iguchi, K.; Yamaotsu, N.; Sugawara, A.; Noguchi, Y.; Saito, Y.; Yamamoto, T.; Watanabe, T.; Shiomi, K.; Ōmura, S.; Hirono, S. NMR spectroscopy and computational analysis of interaction between *Serratia marcescens* chitinase B and a dipeptide derived from natural-product cyclopentapeptide chitinase inhibitor argifin. *Bioorg. Med. Chem.* **2010**, *18*, 5835−5844.

(48) Hirose, T.; Kasai, T.; Akimoto, T.; Endo, A.; Sugawara, A.; Nagasawa, K.; Shiomi, K.; Ōmura, S.; Sunazuka, T. Solution-phase total synthesis of the hydrophilic natural product argifin using 3,4,5-tris(octadecyloxy)benzyl tag. *Tetrahedron* **2011**, *67*, 6633−6643.

(49) Wakasugi, M.; Gouda, H.; Hirose, T.; Sugawara, A.; Yamamoto, T.; Shiomi, K.; Sunazuka, T.; Ōmura, S.; Hirono, S. Human acidic mammalian chitinase as a novel target for anti-asthma drug design using in silico screening. *Bioorg. Med. Chem.* **2013**, *21*, 3214−3220.

(50) Hirose, T.; Maita, N.; Gouda, H.; Koseki, J.; Yamamoto, T.; Sugawara, A.; Nakano, H.; Hirono, S.; Shiomi, K.; Watanabe, T.; Taniguchi, H.; Sharpless, K. B.; Ōmura, S.; Sunazuka, T. Observation of the controlled assembly of preclick components in the in situ click chemistry generation of a chitinase inhibitor. *Proc. Natl. Acad. Sci. U.S.A.* **2013**, *110*, 15892−15897.

(51) Hirose, T.; Sunazuka, T.; Ōmura, S. Recent development of two chitinase inhibitors, argifin and argadin, produced by soil microorganisms. *Proc. Jpn. Acad., Ser. B* **2010**, *86*, 85−102.

(52) Gouda, H.; Sunazuka, T.; Yoshida, K.; Sugawara, A.; Sakoh, Y.; Ōmura, S.; Hirono, S. Three-dimensional solution structure of EM703 with potent promoting activity of monocyte-to-macrophage differentiation. *Bioorg. Med. Chem. Lett.* **2006**, *16*, 2496−2499.

(53) See Supporting Information for more detail.

(54) Hirschmann, R.; Nicolaou, K. C.; Pietranico, S.; Salvino, J.; Leahy, E. M.; Sprengeler, P. A.; Furst, G.; Smith, A. B., III; Strader, C. D.; Cascieri, M. A.; Candelore, M. R.; Donaldson, C.; Vale, W.; Maechler, L. Nonpeptidal peptidomimetics with β-D-glucose scaffolding. A partial somatostatin agonist bearing a close structural relationship to a potent, selective substance P antagonist. *J. Am. Chem. Soc.* **1992**, *114*, 9217−9218.

(55) Hirschmann, R.; Nicolaou, K. C.; Pietranico, S.; Leahy, E. M.; Salvino, J.; Arison, B.; Cichy, M. A.; Spoors, P. G.; Shakespeare, W. C.; Sprengeler, P. A.; Hamley, P.; Smith, A. B., III; Reisine, T.; Raynor, K.; Maechler, L.; Donaldson, C.; Vale, W.; Freidinger, R. M.; Cascieri, M. R.; Strader, C. D. De novo design and synthesis of somatostatin nonpeptide peptidomimetics utilizing and D-glucose as a novel scaffolding. *J. Am. Chem. Soc.* **1993**, *115*, 12550−12568.

(56) Randolph, J. T.; Waid, P.; Nichols, C.; Sauer, D.; Haviv, F.; Diaz, G.; Bammert, G.; Besecke, L. M.; Segreti, J. A.; Mohning, K. M.; Bush, E. N.; Wegner, C. D.; Greer, J. Nonpeptide luteinizing hormone-releasing hormone antagonists derived from erythromycin A: design, synthesis, and biological activity of cladinose replacement analogues. *J. Med. Chem.* **2004**, *47*, 1085−1097.

(57) Oyelere, A. K.; Chen, P. C.; Guerrant, W.; Mwakwari, S. C.; Hood, R.; Zhang, Y.; Fan, Y. Non-peptide macrocyclic histone deacetylase inhibitors. *J. Med. Chem.* **2009**, *52*, 456−468.

(58) Mwakwari, S. C.; Guerrant, W.; Patil, V.; Khan, S. I.; Tekwani, B. L.; Gurard-Levin, Z. A.; Mrksich, M.; Oyelere, A. K. Non-peptide macrocyclic histone deacetylase inhibitors derived from tricyclic ketolide skeleton. *J. Med. Chem.* **2010**, *53*, 6100−6111.

(59) LeMahieu, R. A.; Carson, M.; Kierstead, R. W. A facile preparation of erythronolide A oxime. *J. Antibiot.* **1975**, *28*, 704.

(60) Toshima, K.; Nozaki, Y.; Mukaiyama, S.; Tamai, T.; Nakata, M.; Tatsuta, K.; Kinoshita, M. Application of highly stereocontrolled glycosidations employing 2,6-anhydro-2-thio sugars to the syntheses of erythromycin A and olivomycin A trisaccharide. *J. Am. Chem. Soc.* **1995**, *117*, 3717−3727.

(61) Sun, C.-M.; Shey, J.-Y. High-throughput synthesis of Boc-substituted amidinoureas by liquid-phase approach. *J. Comb. Chem.* **1999**, *1*, 361−363.

(62) Tornøe, C. W.; Christensen, C.; Meldal, M. Peptidotriazoles on solid phase: [1,2,3]-triazoles by regiospecific copper(I)-catalyzed 1,3-dipolar cycloadditions of terminal alkynes to azides. *J. Org. Chem.* **2002**, *67*, 3057−3064.

(63) Rostovtsev, V. V.; Green, L. G.; Fokin, V. V.; Sharpless, K. B. A stepwise huisgen cycloaddition process: copper(I)-catalyzed regioselective "ligation" of azides and terminal alkynes. *Angew. Chem., Int. Ed.* **2002**, *41*, 2596−2599.

(64) National Committee for Clinical Laboratory Standards. Performance standards for antimicrobial disk and dilution susceptibility tests for bacteria isolated from animals. Approved standard M31-A. NCCLS: Wayne, PA, 1999.

(65) van Aalten, D. M. F.; Komander, D.; Synstad, B.; Gaseidnes, S.; Peter, M. G.; Eijsink, V. G. H. Structural insights into the catalytic mechanism of a family 18 exo-chitinase. *Proc. Natl. Acad. Sci. U.S.A.* **2001**, *98*, 8979−8984.

(66) Cornell, W. D.; Cieplak, P.; Bayly, C. I.; Gould, I. R.; Merz, K. M., Jr.; Ferguson, D. M.; Spellmeyer, D. C.; Fox, T.; Caldwell, J. W.; Kollman, P. A. A second generation force field for the simulation of proteins, nucleic acids, and organic molecules. *J. Am. Chem. Soc.* **1995**, *117*, 5179−5197.

(67) Winn, M. D.; Ballard, C. C.; Cowtan, K. D.; Dodson, E. J.; Emsley, P.; Evans, P. R.; Keegan, R. M.; Krissinel, E. B.; Leslie, A. G. W.; McCoy, A.; McNicholas, S. J.; Murshudov, G. N.; Pannu, N. S.; Potterton, E. A.; Powell, H. R.; Read, R. J.; Vagin, A.; Wilson, K. S. Overview of the CCP4 suite and current developments. *Acta Crystallogr., Sect. D: Biol. Crystallogr.* **2011**, *67*, 235−242.

(68) Emsley, P.; Lohkamp, B.; Scott, W. G.; Cowtan, K. Features and development of Coot. *Acta Crystallogr., Sect. D: Biol. Crystallogr.* **2010**, *66*, 486−501.

(69) Lebedev, A. A.; Young, P.; Isupov, M. N.; Moroz, O. V.; Vagin, A. A.; Murshudov, G. N. JLigand: a graphical tool for the CCP4 template-restraint library. *Acta Crystallogr., Sect. D: Biol. Crystallogr.* **2012**, *68*, 431−440.

DOI: 10.1021/acs.jmedchem.5b00175
J. Med. Chem. XXXX, XXX, XXX−XXX